Treading Geodesic Pathways in the Configuration Space of a Linear Polymer

BROWN

Artur Avkhadiev

Brown University

Department of Physics

A thesis submitted for the degree of

Sc.B Honors, Mathematical Physics

May 2018

To my first physics teacher, Alexey Somov.

Acknowledgements

Abstract

In this work, we present a report on the work in progress to develop a geodesic path-finding algorithm for a system of a single linear polymer. To do so, we review the theory of geodesic pathways in the potential energy landscape ensemble and introduce the simple model for a linear polymer: a freely-jointed rigid chain. We show that even without potential energy interactions, the equations of motion for the polymer are complicated due to the constraints on the lengths of the chain links. However, we realize that the path-finding algorithms only requires a short segment along the path that solves these equations motion, not the entire path. We then attempt to obtain a solution that is exact in the limit of a short step, and test our approach using a molecular dynamics simulation. In the end, we analyze the results and formulate directions for further work.

Contents

List of Figures

Chapter 1

Introduction

In trying to understand the dynamics of chemical systems, the analogy with chemical pathways is often invoked: that a system begins and ends in a local minimum of the potential energy, and that the path between the two points is defined by trying to keep activation energy as low as possible. How high a potential energy barrier the system has to surmount defines the slowness of its molecular motion.

There is an alternative to this perspective. The system may evolve not by slowly treading through the potential energy barriers, but by going around those barriers. Then the slowness of molecular motion is defined not by the barriers the system overcomes, but by the long and convoluted — and, in some sense, optimal — pathways it follows to circumvent them.

The idea that these *optimal pathways* can define the rate of molecular motion was pioneered by Chengju Wang and Richard M. Stratt in the context of liquids, supercooled liquids, and glassy systems. They developed the necessary theoretical framework and presented a proof-of-concept by proposing and implementing an algorithm to compute the extended pathways for a simple atomic liquid and a binary glass-forming atomic mixture. [1, 2]

Stratt and collaborators have since fruitfully applied their framework and extended their pathway-finding algorithm to a number of chemical systems, including a liquid of linear molecules, isotropic- and nematic-phase liquid crystals, and roaming motion in the dissociation of formaldehyde. ([3–6]).

This thesis is a work-in-progress report on the extension of the pathway-finding algorithm to linear polymers: long-chain molecules composed of smaller repeating parts. We begin by reviewing the relevant theoretical framework in chapter 2. We then introduce the chemical system under study — linear polymers — and describe the model of a linear polymer we use in our studies in chapter 3. Finally, we report on the development of the

pathway-finding algorithm for linear polymers in chapter 4. In appendix A, we provide an extensive discussion of the ancillary molecular dynamics simulation developed specifically for this problem. Details of the calculations concerning the kinetic energy of the polymer are in appendix B

Chapter 2

Pathways through the Potential Energy Landscape

To appreciate the elegance of the pathway approach, we ought to start with some formalism of classical mechanics that will allow us to generally describe diffusive molecular motion using equations of motion. In section 2.1, we will introduce the discuss the path integral formalism in chemical physics, and how one can think of finding the path described by the equations of motion as a minimization problem in the space of all possible paths the system could take.

This exposition will motivate the framework introduced by [1]: the potential energy landscape ensemble. In section 2.2, we will show how for large systems well-described by classical statistical mechanics, the problem of finding the optimum path can be greatly simplified and generalized within classes of systems with vastly different physical interactions. We will show that the optimal paths we find in the potential energy landscape ensemble are, in a sense, shortest paths, or geodesics.

In section 2.3, we will finally outline how one can, within the framework of the potential energy landscape ensemble, compute the optimal path for a macroscopic system given only where the path begins and ends, and its temperature or an analogous scalar parameter.

2.1 Path-Integral Approach to Diffusion

Diffusion refers to a net random motion of molecules or atoms in a chemical system. The net effect is that of the gradual "spreading out" of molecules or atoms over time — like the melting of a sugar cube in a cup with hot water, or the the smell of fresh coffee wafting evenly to every corner of the room.

We are aiming to describe diffusive motion analytically, and we shall start with a very simple case of free diffusion of point-like particles in a three-dimensional space, ignoring any interactions between the particles. We will follow the development from [7].

It is an experimental observation that particle current $\boldsymbol{j}(\boldsymbol{r}, t)$ is linearly proportional to the spatial variation of particle concentration, c:

$$\boldsymbol{j}(\boldsymbol{r}, t) = -D\boldsymbol{\nabla}c$$

where D is the *coefficient of diffusion*. Larger D implies faster molecular motion. It will play an important role in the subsequent development of the formalism.

An important constraint to impose is that particles are neither destroyed nor created during the diffusive process. This means that the change in particle concentration over time is uniquely determined by spatial variations of particle current:

$$\frac{\partial c}{\partial t} = -\boldsymbol{\nabla} \cdot \boldsymbol{j}$$

As a consequence of the two statements above, we obtain the equation for free diffusion:

$$\frac{\partial c}{\partial t} = -D\nabla^2 c \tag{2.1}$$

To solve this equation, we need to specify initial conditions: the value of the concentration at some time t_0. Consider that at t_0, all particles are at the same point in space $\boldsymbol{r}_0$:

$$c(\boldsymbol{r}, t_0) = \delta(\boldsymbol{r} - \boldsymbol{r}_0),$$

Beginning with this initial condition, the dynamics of the system is governed by equation 2.1. The particles will diffuse away from $\boldsymbol{r}_0$ much like a drop of die spreads out in a cup of water. Given the initial concentration $\delta(\boldsymbol{r} - \boldsymbol{r}_0)$ at t_0, we can interpret $c(\boldsymbol{r}, t)$ for later times as a probability density to find particles that diffused from $\boldsymbol{r}_0$ to $\boldsymbol{r}$ in time $t - t_0$. We denote this probability density as $G\left(\boldsymbol{r}_0 \to \boldsymbol{r} \mid t - t_0\right)$. It is a solution to our equation 2.1, subject to the boundary conditions just discussed:

$$G\left(\boldsymbol{r}_0 \to \boldsymbol{r} \mid t - t_0\right) = \left(4\pi D(t - t_0)\right)^{-\frac{3}{2}} \exp\left(-\frac{(\boldsymbol{r} - \boldsymbol{r}_0)^2}{4D(t - t_0)}\right), \ (t > t_0) \tag{2.2}$$

where the factor of $-\frac{3}{2}$ comes from the total of 3 degrees of freedom our system possesses. The solution may be verified by substitution (see [7]).

Consider a point $(\boldsymbol{r}', t')$, $t' > t_0$. If the function $G\left(\boldsymbol{r}_0 \to \boldsymbol{r}' \mid t' - t_0\right)$ does not vary significantly over some small volume $\int \mathrm{d}\boldsymbol{r}$ containing $\boldsymbol{r}'$, then $\int G\left(\boldsymbol{r}_0 \to \boldsymbol{r}' \mid t' - t_0\right) \mathrm{d}\boldsymbol{r}$ gives the probability for a particle, having started at $\boldsymbol{r}_0$ at the time t_0, to end up in $\int \mathrm{d}\boldsymbol{r}$ at the time t'.

4

Because the microscopic thermal motion leading to diffusion is random, there are many ways the particle can move from $(\boldsymbol{r}_0, t_0)$ to $(\boldsymbol{r}', t')$. And the higher the coefficient of diffusion D — for example, the higher the temperature or the lighter the particles — the more chaotic the motion is going to look like.

We can thus think of infinitely many paths $\boldsymbol{r}(\tau)$, where τ is a parameter along the path ranging from 0 to 1 with $\boldsymbol{r}(0) = \boldsymbol{r}_0$ and $\boldsymbol{r}(1) = \boldsymbol{r}'$. We can then try to construct probability density in the space of paths with an infinitesimal volume element that we denote $\mathcal{D}(\boldsymbol{r}(\tau))$. It makes physical sense, although the math has to follow.

We adopt the construction from Wiegel [7] as follows. We take the entire τ-range from 0 to 1 and divide it into N equal intervals of length $\delta\tau = \frac{1}{N}$. We then ask for a probability density to diffuse from $\boldsymbol{r}(0) = \boldsymbol{r}_0$ to $\boldsymbol{r}(1) = \boldsymbol{r}_N$ in such a way so that the path from $\boldsymbol{r}(0)$ to $\boldsymbol{r}(1)$ also passes through intermediate points $\boldsymbol{r}_1, \boldsymbol{r}_2, \ldots, \boldsymbol{r}_{N-1}$ at $\tau = \frac{1}{N}, \frac{2}{N}, \ldots, \frac{N-1}{N}$, respectively. Since the successive events are independent, the answer is the product of probability densities:

$$\prod_{j=1}^{N} G\left(\boldsymbol{r}_{j-1} \to \boldsymbol{r}_j \mid \frac{j}{N} - \frac{j-1}{N}\right) = \left[(4\pi D\delta\tau)^{-\frac{3}{2}}\right]^N \exp\left(-\frac{1}{4D\delta\tau} \sum_{j=1}^{N} (\boldsymbol{r}_j - \boldsymbol{r}_{j-1})^2\right)$$

Which is the probability for a particle to follow some path $\boldsymbol{r}(\tau), 0 \leq \tau \leq 1$ such that $\boldsymbol{r}(\frac{j}{N}) = \boldsymbol{r}_j, 1 \leq j \leq N-1$. To recover the full probability density of diffusion between $\boldsymbol{r}(0)$ and $\boldsymbol{r}(1)$, we have to integrate the N intermediate points over space. Defining

$$\int \mathcal{D}(\boldsymbol{r}(\tau)) = \left[(4\pi D\delta\tau)^{-\frac{3}{2}}\right]^N \prod_{j=1}^{N-1} \int_{-\infty}^{+\infty} \mathrm{d}\boldsymbol{r}_j \tag{2.3}$$

and

$$\exp\left(-\frac{1}{4D} \int_0^1 \left(\frac{\mathrm{d}\boldsymbol{r}}{\mathrm{d}\tau}\right)^2 \mathrm{d}\tau\right) = \exp\left(-\frac{1}{4D\delta\tau} \sum_{j=1}^{N} (\boldsymbol{r}_j - \boldsymbol{r}_{j-1})^2\right) \tag{2.4}$$

we perform the integration over the intermediate points, and *then* take the limit of $N \to \infty$. Finally, we obtain what's called the Wiener integral:

$$G\left(\boldsymbol{r}_0 \to \boldsymbol{r} \mid t - t_0\right) = \int_{\boldsymbol{r}(0)}^{\boldsymbol{r}(1)} \mathcal{D}(\boldsymbol{r}(\tau)) \exp\left(-\frac{1}{4D} \int_0^1 \left(\frac{\mathrm{d}\boldsymbol{r}}{\mathrm{d}\tau}\right)^2 \mathrm{d}\tau\right) \tag{2.5}$$

which is a path integral formulation for the solution we already obtained in equation 2.2. The exponent in the integrand acts as a probability weight, much like the more familiar Boltzmann weight in statistical mechanics. The closer the weight the 1, the more likely the path. In that sense, the path integral is akin to a partition function in statistical mechanics.

In our particular case — *free* diffusion — the integral in the exponent of the integrand is nothing other than the action S. In classical dynamics, S is equal to

$$S = \int_a^b L(q(\tau), \dot{q}(\tau), \tau) \, \mathrm{d}\tau$$

where L is a Lagrangian. A Lagrangian can depend on the generalized coordinates q and their time derivatives $\dot{q}$. Equations of motion in classical mechanics — the functions $q(\tau)$ — are derived from the least action principle: a condition that requires that functions $q(\tau)$ extremize the functional S. This condition is equivalent to Euler-Lagrange equations:

$$\frac{\mathrm{d}}{\mathrm{d}\tau}\left(\frac{\partial L}{\partial \dot{q}}\right) - \frac{\partial L}{\partial q} = 0 \tag{2.6}$$

Together with boundary values or initial conditions, Euler-Lagrange equations allow to solve for classical equations of motion. Since classical equations of motion minimize the action, they will also attain the highest probability weight in equation 2.5. From a saddle point approximation of the integral, we can therefore see that the optimal paths will dominate the system in the limit of slow diffusion ($D \to 0$), while other paths will die out exponentially. Wang and Stratt [2] show that one can think of the optimal paths geometrically as centroids of the paths one would observe when diffusion is slow, and may wonder whether studying the statistics of optimal paths in this regime offer any insights into the system dynamics. Of course, to study optimal paths, one first needs to know how to obtain them.

In the simple problem we considered, we ignored all interactions between particles. The interactions between atoms and molecules are, of course, the crux of a physical problem for any chemical system of interest. And for any real system, the details of those interactions are quite complicated. Including potential energy considerations into the problem of diffusion can drastically modify the exponent of the integrand in equation 2.5.[1] It would be very hard to find optimal paths from the resulting path integrals. Unless we are able to generalize the problem of finding optimal paths in such a way so that potential energy does not present these challenges, attempting to study the dynamics of chemical systems via the statistics of optimal paths is untenable.

2.2 The Potential Energy Landscape

At this point the theoretical framework developed by Wang and Stratt [1] comes into play. The path integral 2.5 is analogous to a partition function in statistical mechanics:

---

[1]With diffusion problems, the integrand's exponent is *not* an action from classical dynamics. Generally, one has to start with an equation like the one we wrote for free diffusion (2.1) but also consider the interactions between the molecules. For example, see the Fokker-Planck equation and the corresponding path integrals.[8]

each path is a succession of microscopic configurations

$$\boldsymbol{R} = (\boldsymbol{r}_0,\, \boldsymbol{r}_1,\, \ldots,\, \boldsymbol{r}_{N-1},\, \boldsymbol{r}_N)$$

with corresponding complicated potential energies, and to each microscopic configuration we need to assign a probability weight. In systems with potential energy interactions, that weight does *not* look like the exponential in the integrand of equation 2.5; it is significantly more complicated (for example, see the path-integral formulation for the Fokker-Planck equation in [8]). Given the probability weighting, some successions of configurations $\boldsymbol{R}(\tau)$ will be more likely than others. In this way, a probability distribution over microscopic configurations will give rise to the system's macroscopic behavior.

Points ($\boldsymbol{R}$) can be imagined to inhabit an abstract multidimensional space called a configuration space. The number of dimensions in this space is equal to the number of coordinates — physically, we can think of these coordinates as representing positions of particles. Each point in configuration space corresponds to a microscopic configuration.

It is a central result of classical statistical mechanics that in systems with a large number of elements, there can be many equivalent ways of bookkeeping the probabilities assigned to microscopic states that give rise to the correct macroscopic physical behavior. These bookkeeping systems are called statistical *ensembles*.

An ensemble defines an aggregate of allowed microscopic states. For example, an ensemble may include all possible microscopic states at the same energy. In that case, one invokes the maximum entropy principle to derive the underlying probability distribution over the allowed states.[1] So long as the system in question is large (formally, the number of elements $N \to \infty$), all well-defined statistical ensembles are equivalent, giving rise to the same macroscopic behavior.

Wang and Stratt [1] developed a statistical ensemble that immensely simplifies the problem of finding optimal paths despite a possibly complicated potential energy weighting. Given a fixed upper limit on potential energy, called the landscape energy E_L, the ensemble considers all microscopic states whose potential energy is at or below the landscape energy. They derive the resulting probability density to be:

$$\rho(\boldsymbol{R}) = \frac{\theta(E_L - U(\boldsymbol{R}))}{\int \mathrm{d}\boldsymbol{R}\,\theta(E_L - U(\boldsymbol{R}))} \tag{2.7}$$

where $\theta(x)$ is a step function, $\theta(x) = \begin{cases} 1, & x \geq 0 \\ 0, & x < 0 \end{cases}$. This density assigns a probability of 0 to all configurations with potential energy above the landscape energy, distributing probability equally among all other configurations.

Because all well-defined ensembles are equivalent in the limit as the system gets large, the landscape energy E_L corresponds to physical quantities held fixed in other ensembles, like

temperature. The landscape energy is therefore not set arbitrarily, but rather corresponds to the physical regime in which we want to study a given chemical system.

With this way of bookkeeping the probabilities, the integrand in equation 2.5 vanishes whenever the potential energy of a configuration exceeds the specified landscape energy E_L. In configurations where the potential energy is at or below E_L, the potential energy does not change the probability weight. In effect, the potential energy landscape ensemble allows us to frame the general problem of computing optimal paths as that of free diffusion with an inequality constraint on the potential energy. We are to minimize the action:

$$\begin{cases} \delta S = \delta \int_0^1 T \, \mathrm{d}\tau = 0, & \text{subject to a constraint} \\ U \leq E_L. \end{cases} \tag{2.8}$$

where T is the kinetic energy of the system. Since T is a non-negative function, it is easy to see that minimizing the integral in 2.8 is equivalent to minimizing

$$\ell = \int_0^1 \sqrt{2T} \, \mathrm{d}\tau \tag{2.9}$$

To understand the meaning of ℓ, consider the familiar case of an atomic liquid, where $T = \frac{1}{2} m \left(\frac{\mathrm{d}\boldsymbol{R}}{\mathrm{d}\tau} \right)^2$. We can see that

$$\ell = \int_0^1 \sqrt{m \left(\frac{\mathrm{d}\boldsymbol{R}}{\mathrm{d}\tau} \right)^2} \, \mathrm{d}\tau = \int_0^1 \sqrt{m} \, \|\mathrm{d}\boldsymbol{R}\|, \tag{2.10}$$

a quantity that is clearly proportional to the length of the path. Generally, we shall call $\ell = \int_0^1 \sqrt{2T} \, \mathrm{d}\tau$ a *kinematic length*.

We are finally able to appreciate the utility of the potential energy landscape ensemble. In that ensemble, an optimal path between two points in configuration space of the system can be computed as the shortest path, or a geodesic, in the sense of minimizing its kinematic length, subject to the constraint that the potential energy does not exceed E_L anywhere along the path. The statistical properties of geodesics in a given system — for example, the distribution of their length — can in turn be used to study diffusion in the system. We have thus connected the *geometry* of the potential energy landscape with the *dynamics* of the system under study.

2.3   Computing the Optimal Pathways in the Potential Energy Landscape Ensemble

So far, we have greatly simplified the problem of finding optimal paths and discovered the geometric significance of the problem's solution in the potential energy landscape

ensemble. But given the starting and ending point for a path in configuration space, how do we go about actually computing a landscape geodesic?

Crucially, we are solving a minimization problem with inequality constraints, summarized in equation 2.8. The key piece of mathematics that we need is the Kuhn-Tucker optimization theorem.[2] As a consequence of the theorem, the geodesic, a solution to the minimization problem with inequality constraints, is a union of paths that satisfy 2.8 without the constraint, and paths that satisfy 2.8 when the constraint is the exact equality, $U = E_L$.

Given the boundary values in configuration space and the Kuhn-Tucker theorem, we can devise a strategy that allows us to otbain a path of the same class as the geodesic: a union of off-boundary and on-boundary segments. An outline of the procedure is as follows:

1. Set the current position to one of the endpoints.

2. Starting at the current position, make a short step in configuration space along the off-boundary geodesic between the current position and the endpoint: that is, solve the Euler-Lagrange equations without the potential energy constraint.

3. If the obtained configuration has the potential energy at or below E_L, it becomes our current position and we make another short step from there; if the potential energy is greater than E_L, we escape to an allowed configuration using a yet-to-be devised method.

4. Continue on until the path is as close to the final endpoint as desired.

The procedures for making steps off-boundary or escaping back to allowed configurations may vary from problem to problem, and the solution obtained in the end is not necessarily a geodesic. Once we obtain the path, we need to see if small modifications to it yield a path that is shorter. This optimization stage may be done using Monte-Carlo methods.

In this thesis, we discuss the progress made for the off-boundary solutions for a system of one linear polymer. We follow up with a brief discussion of the system under study in chapter 3 before we discuss the development of the algorithm in chapter 4.

Chapter 3

Linear Polymers

3.1 Polymers and their Models

Polymers are long-chain molecules composed of identical repeating units called monomers. Polymers are ubiquitous both in nature and chemical synthesis. Polysaccharides and cellulose are examples of biopolymers. Synthetic polymers include such brand-name materials as nylon, Kevlar™, and Teflon™.

Monomers forming a polymer are chained together with chemical bonds. The number of monomers in a polymer can get extremely large. In fact, an entire macroscopic sample of a chemical substance like rubber can be considered a single polymer. The chain of monomers can be linear or have branches, but structurally there is always the main longest chain called a backbone.[9]

This impressive chemical and structural diversity of polymers affords the diversity of their dynamics. Whether it is chain-folding in proteins or phase transitions in rubber, intricate dynamics arise from the interplay of polymer structure, size, and chemical interactions.[10, 11]

If we wish to study polymer dynamics, we need a physical model. How good the model is depends on the research goals. The more specific it is to a particular class of polymers, the more specific its dynamical predictions will be. Of course, it is impossible that, say, protein and rubber dynamics are described an identical set of rules. Still, there may be a small set of principles governing all polymer dynamics, regardless of the details of their structure and chemical interactions. If we seek to study these general principles, we need to abstract our model away from the details of any particular polymer. To quote the famous mathematician George E. P. Box, "All models are wrong; some models are useful."[12]

In this work, we aim to extend the framework of landscape geodesics to polymers generally. In doing so, we need a model that captures the essential features of any polymer.

3.2 Freely-Jointed Chain as a Model for Linear Polymers

Essentially, all polymers are chains. Our model is also a chain — the most simple chain one could imagine. The chain is linear (i.e., not branched) and consists of identical links of fixed size connected by identical atoms. The chain is freely jointed: there are no structural constraints on how a link should rotate around the atoms connecting it to other links.

To speak of the size of the atoms or length of the links joining them, we should first identify the relevant units. These units are imposed by the physical potential of our choice. For example, it does not make sense to say that atoms in the chain are close to or far away from each other without referencing the relevant length scale, but it does make sense to say they are close if at that separation they are strongly repelled by the potential forces.

We choose to model the interactions between the atoms in the polymer with a Lennard-Jones potential. Given the length of the separation vector between atoms labeled a and b, $\boldsymbol{r}_{ab}$, the Lennard-Jones pair potential is given by:

$$u^{\mathrm{LJ}}(\boldsymbol{r}_{ab}) = 4\varepsilon \left[\left(\frac{\sigma}{\boldsymbol{r}_{ab}} \right)^{12} - \left(\frac{\sigma}{\boldsymbol{r}_{ab}} \right)^{6} \right] \tag{3.1}$$

Lennard-Jones potential is often used in molecular dynamics simulations because it is both simple and captures the essential features of interatomic potentials: strong repulsion at $r_{ab} < \sigma$, $u^{\mathrm{LJ}} = 0$ at $r_{ab} = \sigma$, followed by a potential well of depth $u^{\mathrm{LJ}} = -\epsilon$ at $r_{ab} = \sigma\sqrt[6]{2}$, and approaching 0 again as $r_{ab} \to \infty$. Here, ε defines the relevant energy scale and σ defines the relevant length scale. σ can be thought of as an effective diameter of our atoms. Since there is only one kind of atom in our model, we can use the atomic mass to define mass units. Having fixed the units of mass, length, and energy, we can derive other relevant scales like the time scale. [13].

Since the length of each link is fixed, the total potential energy U of the polymer is given by the sum of pairwise interactions betwen its non-neighboring atoms. The kinetic energy T of the polymer is the sum of kinetic energies of its atoms. For a linear polymer with

N links,

$$U = \sum_{\substack{a=0 \\ b=a+2}}^{N} u^{\mathrm{LJ}}(\boldsymbol{r}_{ab})$$

$$T = \sum_{a=0}^{N} \frac{m\boldsymbol{v}_a^2}{2}$$

(3.2)

Here, we are using $N+1$ atomic positions $\boldsymbol{r}$ and velocities $\boldsymbol{v}$ in the lab frame to describe the state of the polymer. The configuration space vector is $\boldsymbol{R}_{\mathrm{atm}} = (\boldsymbol{r}_0,\ \boldsymbol{r}_1,\ \ldots,\ \boldsymbol{r}_{N-1},\ \boldsymbol{r}_N)$ — call it the atomic-position representation. Equivalently, we can describe the configuration of our polymer using the N unit vectors $\hat{\boldsymbol{\Omega}}$ directed along each of its links together with the position of the center of mass $\boldsymbol{r}_{\mathrm{CM}}$. In this case, $\boldsymbol{R}_{\mathrm{lnk}} = (\boldsymbol{r}_{\mathrm{CM}},\ \hat{\boldsymbol{\Omega}}_1,\ \hat{\boldsymbol{\Omega}}_2,\ \ldots,\ \hat{\boldsymbol{\Omega}}_{N-1},\ \hat{\boldsymbol{\Omega}}_N)$. We call it the link-vector representation. The two representations are summarized on figure 3.1.

The two representations are interconvertible given the fixed length of each link, which we denote d. Each unit link vector $\hat{\boldsymbol{\Omega}}_k$ is directed parallel to the bond between atoms $k-1$ and k and points towards the atom with the larger index:

$$\hat{\boldsymbol{\Omega}}_k = \frac{\boldsymbol{r}_k - \boldsymbol{r}_{k-1}}{\|\boldsymbol{r}_k - \boldsymbol{r}_{k-1}\|}$$

(3.3)

Because the length of each link is fixed, the time derivative $\dot{\hat{\boldsymbol{\Omega}}}$ describes the rotational motion of each link.[1]

Since the mass of each atom in the polymer is the same, the position of the center of mass $\boldsymbol{r}_{\mathrm{CM}}$ is given by

$$\boldsymbol{r}_{\mathrm{CM}} = \frac{1}{N+1}\left(\sum_{a=0}^{N} \boldsymbol{r}_a\right)$$

(3.4)

Together with the constraints on the distance between neighboring atoms, we can use equations 3.3 and 3.4 to obtain inverse maps $\boldsymbol{r}(\boldsymbol{r}_{\mathrm{CM}}, \{\hat{\boldsymbol{\Omega}}_k \mid k = 1, \ldots, N\})$. In turn, these functions give the kinetic energy of the polymer as a function of $\boldsymbol{v}_{\mathrm{CM}}$ and $\{\dot{\hat{\boldsymbol{\Omega}}}_k\}$:

$$T = \frac{1}{2}(N+1)m\boldsymbol{v}_{\mathrm{CM}}^2 + \frac{1}{2}I_0 \sum_{k,\,l=1}^{N} D_{kl}\left(\dot{\hat{\boldsymbol{\Omega}}}_k \cdot \dot{\hat{\boldsymbol{\Omega}}}_l\right)$$

(3.5)

where $I_0 = md^2$ and the dyadic product $I_0 \sum_{k,\,l=1}^{N} D_{kl}\left(\hat{\boldsymbol{\Omega}}_k\hat{\boldsymbol{\Omega}}_l\right)$ gives the moment of inertia tensor for a given configuration of the polymer, and the matrix D_{kl} is

$$D_{kl} = \frac{\min(k,\,l)(N+1) - kl}{N+1}$$

(3.6)

_____

[1] *NB*: $\dot{\hat{\boldsymbol{\Omega}}}$ is not a unit vector.
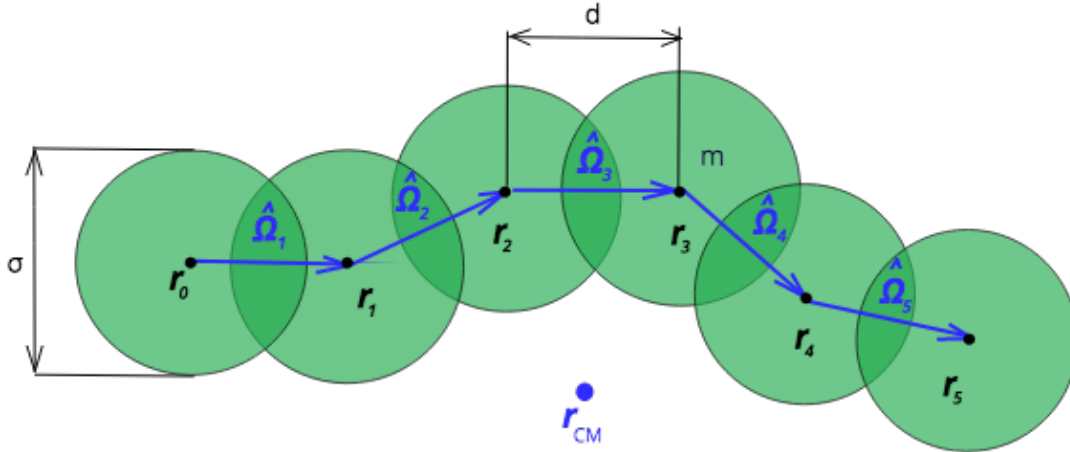
Figure 3.1: The model for a linear polymer used in molecular dynamics simulations and in computing geodesic paths. The configuration space vector has two representations: the atomic-position representation (see equation 3.2) and the link-vector representation (see equation 3.5)

The details of the derivations are provided in appendix B. In the link-vector representation, the kinetic energy is explicitly divided into that of the center of mass motion and that of the motion around the center of mass. We call the latter the internal kinetic energy.

Although the two representations of polymer's configuration are interconvertible, the link-vector representation is more convenient, because it is easier to ensure that the length of each link stays fixed when using $\hat{\boldsymbol{\Omega}}$'s: all we need is to have $\dot{\hat{\boldsymbol{\Omega}}}_k \perp \hat{\boldsymbol{\Omega}}_k \ \forall k$ — then the normalizations of all $\hat{\boldsymbol{\Omega}}$'s are respected. In contrast, atomic velocities $\boldsymbol{v}_a$ require a more elaborate treatment to ensure the normalization constraints are satisfied.

In this work, we use the atom-position representation in molecular dynamics simulations to obtain the endpoints for our geodesics: the initial and final configurations of the polymer when the system is equilibrated. There are known MD algorithms that solve the initial-value problem for equations of motion with constraints such as the ones that we have (see RATTLE in appendix A).

In contrast, when calculating the off-boundary segments of geodesics, we need to solve a *boundary-value* problem for the same equations of motion with constraints. When dealing with geodesics, we work in the link-vector representation. In particular, we use the kinetic energy of the polymer in the form of equation 3.5.

13

Chapter 4

Geodesic Path Finding Algorithm

In this chapter, we discuss in detail the development of the algorithm for computing off-boundary segments of geodesics in the configuration space of a linear polymer. The discussion builds on the theory laid out in section 2.3, adapting the general framework to the particular model described in section 3.2.

We begin by discussing the analogue of kinetic energy in the configuration space and briefly reviewing constrained lagrangian dynamics in section 4.1. The constrained dynamics are required in our model to fix the lengths of the chain links. We then explain the solution for off-boundary geodesic segments for a single link in section 4.2, and finish the chapter by discussing the developments for a multi-link solution in section 4.3.

4.1   Solving for geodesics in general

It is important that the path-propagation algorithm to obtain a geodesic is realized in short steps. At every step of the propagation, we have a current configuration $\boldsymbol{R}^{(m)}$ and the best guess of how the geodesic is going to look like from then on, $\boldsymbol{R}^{m \to f}(\tau)$ — call it the best-guess path. In the potential energy landscape ensemble, the best-guess path is obtained by solving the Euler-Lagrange equations where the Lagrangian does not depend on the potential energy of the system:

$$L = T = \frac{1}{2}m\left(\frac{\mathrm{d}\boldsymbol{R}}{\mathrm{d}\tau}\right)^2$$

The best-guess path exactly coincides with the eventual solution in the absence of potential energy boundaries. In reality, some configurations $\boldsymbol{R}$ may be forbidden because they have a potential energy above the landscape energy E_L. The geodesic solution is not allowed to pass through these forbidden areas of the configuration space — but the best-guess path $\boldsymbol{R}^{m \to f}(\tau)$, being an off-boundary solution, may foray into those areas. The

only way for us to detect and prevent these forays is to propagate the path in incremental steps (indexed m): if the step $m+1$ along $\boldsymbol{R}^{m\to\mathrm{f}}(\tau)$ yields a forbidden configuration, we can escape to the configuration with a low enough potential energy, and make the new guess from there. To ensure that we don't incur too far into a forbidden region and are able to escape successfully, the step along $\boldsymbol{R}^{m\to\mathrm{f}}(\tau)$ has to be small relative to the length scale dictated by the potential. At every step, we update our best guess to ensure we are staying on track.

The meaning of the variable τ, although ostensibly close to that of time, is actually distinct and requires a careful treatment. There is no notion of time in configuration space; a path in the configuration space is only a succession of configurations, with no information about how those configurations are time separated. The only meaningful parameters pertinent to the separation of the configurations along the path are thus concerned with their *spatial* separation. A particularly useful class of such parameters are those that are affinely related with the length of the path ℓ:

$$s = a\ell + b \tag{4.1}$$

The parameter τ we will rely on extensively throughout this chapter is an affine parameter with $b = 0$ for the best-guess path $\boldsymbol{R}^{m\to\mathrm{f}}(\tau)$ from a current position to the final endpoint configuration. And, since the best-guess path is updated at every step, τ is a local parameter. A step $\delta\tau$ measures how close the current configuration $\boldsymbol{R}^{(m)}$ is to the following one, $\boldsymbol{R}^{(m+1)} = \boldsymbol{R}^{m\to\mathrm{f}}(\delta\tau)$.

If, in addition to solving the Euler-Lagrange equations of motion, we want the optimal path to satisfy a number of constraints of the form $\sigma(\boldsymbol{R}, \tau) = 0$ — for example, constraints that fix the length of each polymer link like $\hat{\boldsymbol{\Omega}}_k \cdot \hat{\boldsymbol{\Omega}}_k - 1 = 0$ — then we need to modify the Lagrangian. In particular, this can be done using the method of undetermined Lagrange multipliers. If there are N constraints to satisfy, the Lagrangian becomes:

$$L' = L - \sum_{k=1}^{N} \lambda_k(\tau)\sigma_k(\boldsymbol{R}, \tau) \tag{4.2}$$

Note the fact that Lagrange multipliers λ_k generally depend on τ. Now the optimal path is the solution to the system of equations, including the Euler-Lagrange equations for L' as well as the N constraint equations $\sigma_k(\boldsymbol{R}, \tau) = 0$. For $L = T = \frac{1}{2}m\left(\frac{\mathrm{d}\boldsymbol{R}}{\mathrm{d}\tau}\right)^2$, this system of equations is:

$$\frac{\mathrm{d}^2 R_l}{\mathrm{d}\tau^2} - \sum_{k=1}^{N} \lambda_k(\tau)\frac{\partial\sigma_k}{\partial R_l} = 0$$
$$\sigma_k(\boldsymbol{R}, \tau) = 0 \tag{4.3}$$

where R_l are components of $\boldsymbol{R}$ written in Cartesian coordinates, and $(G_k)_l(\tau) = \sum_{k=1}^{N} \lambda_k(\tau)\frac{\partial\sigma_k}{\partial R^l}$ are components of constraint forces $\boldsymbol{G}_l(\tau)$. At any point along the path, the magnitude

and direction of these forces is such that they ensure the given configuration $\boldsymbol{R}$ respects the constraint equations.

In the molecular dynamics simulation designed for this work, we employ a standard numerical integration scheme that solves the system 4.3 by approximating the constraint forces at each step — see RATTLE in [14] and in appendix A. However, MD simulations solve initial value problems, yielding numerical solutions to EL equations given the initial value of all positions and momenta (a point in phase space). In calculating the geodesics, we have a boundary value problem: we need to find a path between two points in configuration space that solves the system 4.3. Numerical schemes like RATTLE do not seem to work.

The remaining two sections of this chapter address the solution of the system 4.3 with boundary values.

4.2 Solving for off-boundary geodesic segments of a single link

Breaking the problem of multi-link dynamics into bits, it is wise to first understand the motion of a single link by simplifying our Lagrangian 3.5. If we remove cross terms from the internal kinetic energy term, we effectively reduce the dynamics to that of N decoupled diatomic molecules:

$$T = \sum_{k=1}^{N} \left(\frac{1}{2} m \boldsymbol{v}_k^2 + \frac{1}{2} I_0 \frac{\mathrm{d}\hat{\boldsymbol{\Omega}}_k}{\mathrm{d}\tau} \cdot \frac{\mathrm{d}\hat{\boldsymbol{\Omega}}_k}{\mathrm{d}\tau} \right)$$

When the motion is decoupled, it suffices to consider a single link ($N = 1$).

Furthermore, when we eventually consider the motion of a single polymer, we will not be interested in its translational motion. In our molecular dynamics simulations that we use to obtain the path endpoints, we could initialize the polymer with $\boldsymbol{r}_{\mathrm{CM}} = \boldsymbol{0}$ and fix $\boldsymbol{v}_{\mathrm{CM}} = \boldsymbol{0}$. Since the polymer molecules are only interacting among themselves, the center of mass would always stay at the origin, and so all the endpoints we use to compute the geodesics would have $\boldsymbol{r}_{\mathrm{CM}} = \boldsymbol{0}$. Staying at $\boldsymbol{r}_{\mathrm{CM}} = \boldsymbol{0}$ throughout the path would then clearly give the translational component of the geodesic.

We therefore ignore all translational motion of a single link. According to equation 4.2, we want to obtain a geodesic path from the following action

$$S = \int_0^1 \mathrm{d}\tau \, \frac{1}{2} I_0 \left(\frac{\mathrm{d}\hat{\boldsymbol{\Omega}}}{\mathrm{d}\tau} \cdot \frac{\mathrm{d}\hat{\boldsymbol{\Omega}}}{\mathrm{d}\tau} \right)(\tau) - \lambda(\tau) \left(\hat{\boldsymbol{\Omega}}^2(\tau) - 1 \right) \tag{4.4}$$

subject to a constraint

$$\left\|\hat{\boldsymbol{\Omega}}(\tau)\right\| - 1 = 0 \tag{4.5}$$

with the following boundary conditions

$$\hat{\boldsymbol{\Omega}}(0) = \hat{\boldsymbol{\Omega}}^{\text{i}}, \quad \hat{\boldsymbol{\Omega}}(1) = \hat{\boldsymbol{\Omega}}^{\text{f}} \tag{4.6}$$

The solution that the geodesic path for this system satisfies is known in computer graphics as **s**pherical **l**inear int**erp**olation, or Slerp.[15] Starting at $\hat{\boldsymbol{\Omega}}^{\text{i}}$ at $\tau = 0$, the link following the Slerp path will rotate at a constant rate toward $\hat{\boldsymbol{\Omega}}^{\text{f}}$, staying in the plane defined by the two vectors. The link's rotational speed is such that it reaches $\hat{\boldsymbol{\Omega}}^{\text{f}}$ at $\tau = 1$, and is proportional to the angle between initial and final orientations, $\psi = \arccos\left(\hat{\boldsymbol{\Omega}}^{\text{i}} \cdot \hat{\boldsymbol{\Omega}}^{\text{f}}\right)$. The Slerp motion of a single link vector is depicted on figure 4.1

Jacobson and Stratt [3, 4] obtain the Slerp solution from the action 4.4 by parameterizing $\hat{\boldsymbol{\Omega}}$ in terms of its components along $\hat{\boldsymbol{\Omega}}^{\text{i}}$, $\hat{\boldsymbol{\Omega}}^{\text{f}}$, and the unit vector normal to the plane defined by them, $\hat{\boldsymbol{n}} = \frac{\hat{\boldsymbol{\Omega}}^{\text{i}} \times \hat{\boldsymbol{\Omega}}^{\text{f}}}{\left\|\hat{\boldsymbol{\Omega}}^{\text{i}} \times \hat{\boldsymbol{\Omega}}^{\text{f}}\right\|}$:

$$\hat{\boldsymbol{\Omega}}(\tau) = a(\tau)\hat{\boldsymbol{\Omega}}^{\text{i}} + b(\tau)\hat{\boldsymbol{\Omega}}^{\text{f}} + c(\tau)\hat{\boldsymbol{n}} \tag{4.7}$$

subject to constraint 4.11 and boundary conditions 4.12.[3]

After minimizing the action, eliminating the Lagrange multiplier λ and substituting the boundary values, the Slerp solution, which we denote $\hat{\boldsymbol{\Omega}}_{\text{S}}$, is

$$\begin{cases} \hat{\boldsymbol{\Omega}}_{\text{S}}(\tau) = \frac{\sin\left(\psi(1-\tau)\right)}{\sin(\psi)}\hat{\boldsymbol{\Omega}}^{\text{i}} + \frac{\sin(\psi\tau)}{\sin(\psi)}\hat{\boldsymbol{\Omega}}^{\text{f}} \\ \cos\left(\psi\right) = \hat{\boldsymbol{\Omega}}^{\text{i}} \cdot \hat{\boldsymbol{\Omega}}^{\text{f}} \end{cases} \tag{4.8}$$

Parameterized according to equation 4.7, the Slerp solution has $c = 0$. That means the link stays in the plane defined by $\hat{\boldsymbol{\Omega}}^{\text{i}}$ and $\hat{\boldsymbol{\Omega}}^{\text{f}}$ throughout the path.

Since the shortest path is the same going from $\hat{\boldsymbol{\Omega}}^{\text{i}}$ to $\hat{\boldsymbol{\Omega}}^{\text{f}}$ as going from $\hat{\boldsymbol{\Omega}}^{\text{f}}$ to $\hat{\boldsymbol{\Omega}}^{\text{i}}$, the expression 4.8 is invariant under the simultaneous time reversal and exchange of boundary conditions.

The algorithm to obtain the geodesic candidate according to equation 4.8 is iterative. We begin at $\hat{\boldsymbol{\Omega}}_{\text{S}}^{(0)} = \hat{\boldsymbol{\Omega}}^{\text{i}}$ and make a short angular step $\delta\psi = \psi^{(0)}\delta\tau$ along the path toward $\hat{\boldsymbol{\Omega}}^{\text{f}}$, obtaining a new configuration. If the new configuration does not satisfy the inequaility constraint on the potential energy, we follow an escape-step procedure until we obtain a configuration that does. Once we have the configuration that is at or below the landscape energy E_L, we call it $\hat{\boldsymbol{\Omega}}_{\text{S}}^{(1)}$. Then we make another short step, this time following a path
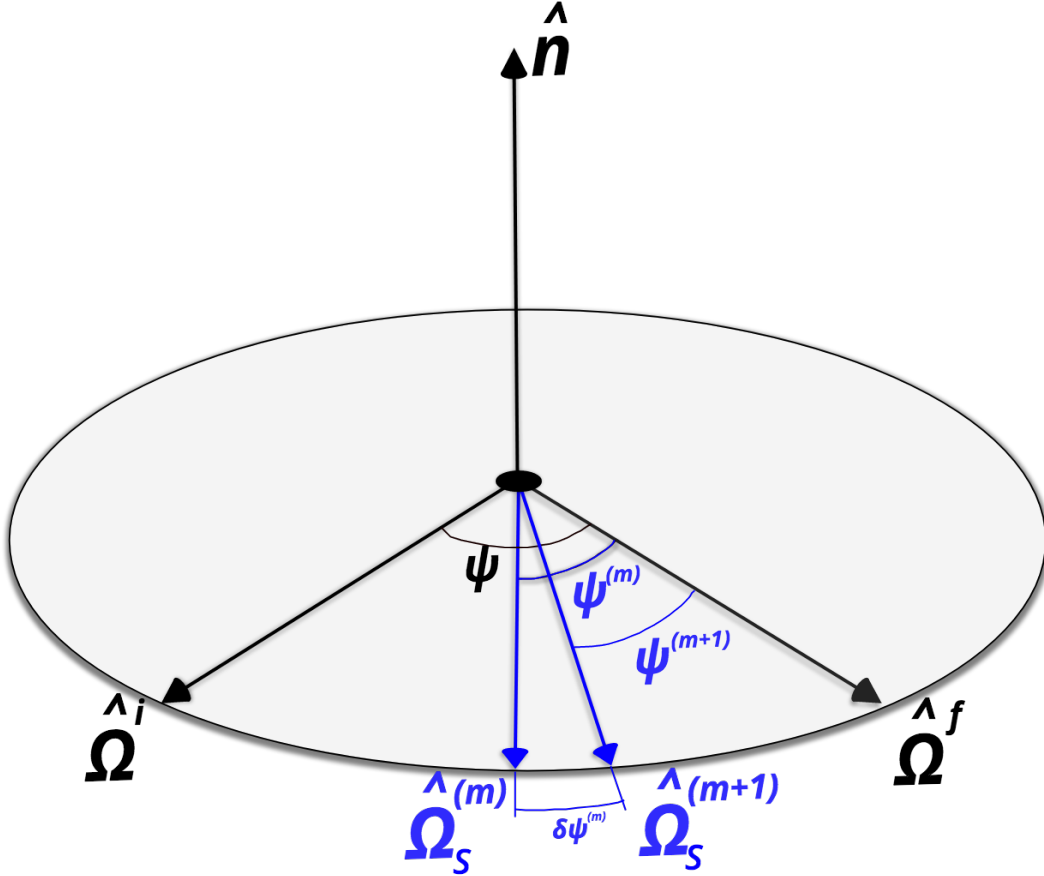
Figure 4.1: A single link vector $\hat{\mathbf{\Omega}}$ moving between $\hat{\mathbf{\Omega}}^{\mathrm{i}}$ and $\hat{\mathbf{\Omega}}^{\mathrm{f}}$ according to the Slerp solution $\hat{\mathbf{\Omega}}_{\mathrm{S}}(\tau)$. In the simulation, the motion is incremental in steps m. Throughout its motion, the link remains in the plane defined by $\hat{\mathbf{\Omega}}^{\mathrm{i}}$ and $\hat{\mathbf{\Omega}}^{\mathrm{f}}$.

from $\hat{\mathbf{\Omega}}_{\mathrm{S}}^{(1)}$ to $\hat{\mathbf{\Omega}}^{\mathrm{f}}$ (the boundary conditions are different). If we do not worry about the potential energy boundaries, the whole process can be summarized as follows:

$$
\begin{cases}
\hat{\mathbf{\Omega}}_{\mathrm{S}}^{(0)} \triangleq \hat{\mathbf{\Omega}}^{\mathrm{i}} \\
\hat{\mathbf{\Omega}}_{\mathrm{S}}^{(m+1)} \triangleq \dfrac{\sin\left(\psi_{\mathrm{S}}^{(m)}(1-\delta\tau)\right)}{\sin\left(\psi_{\mathrm{S}}^{(m)}\right)}\hat{\mathbf{\Omega}}_{\mathrm{S}}^{(m)} + \dfrac{\sin\left(\psi_{\mathrm{S}}^{(m)}\delta\tau\right)}{\sin\left(\psi_{\mathrm{S}}^{(m)}\right)}\hat{\mathbf{\Omega}}^{\mathrm{f}} \\
\cos(\psi_{\mathrm{S}}^{(m)}) \triangleq \hat{\mathbf{\Omega}}_{\mathrm{S}}^{(m)} \boldsymbol{\cdot} \hat{\mathbf{\Omega}}^{\mathrm{f}}
\end{cases}
\tag{4.9}
$$

The entire process is incremental in steps m. This procedure allows us to obtain off-boundary segments of a geodesic candidate for the system whose action is given by equation 4.4. The parameter $\delta\tau$ can be determined in a number of ways, but, given the bond length d, it has to lead a step with arclength $(\psi_{\mathrm{S}}^{(m)}\delta\tau)d$ small compared to the relevant length scale σ.

4.3 Solving for off-boundary geodesic segments of a linear polymer

Once N individual links are coupled together in a linear polymer chain, things get messy. Given a configuration space vector $\boldsymbol{R}_{\text{lnk}} = (\boldsymbol{r}_{\text{CM}}, \hat{\boldsymbol{\Omega}}_1, \hat{\boldsymbol{\Omega}}_2, \ldots, \hat{\boldsymbol{\Omega}}_{N-1}, \hat{\boldsymbol{\Omega}}_N)$, we ignore $\boldsymbol{r}_{\text{CM}}$, restricting our attention to the collection of unit link vectors $\hat{\boldsymbol{\Omega}}_{k=1,\ldots,N}$. The action

$$S = \int_0^1 \mathrm{d}\tau \sum_{k,\,l=1}^N \frac{1}{2} I_0 D_{k,\,l} \left(\frac{\mathrm{d}\hat{\boldsymbol{\Omega}}_k}{\mathrm{d}\tau} \cdot \frac{\mathrm{d}\hat{\boldsymbol{\Omega}}_l}{\mathrm{d}\tau} \right)(\tau) - \sum_{k=1}^N \lambda_k(\tau) \left(\hat{\boldsymbol{\Omega}}_k^2(\tau) - 1 \right) \qquad (4.10)$$

subject to constraints $\forall\, k = 1, \ldots, N$:

$$\left\| \hat{\boldsymbol{\Omega}}_k(\tau) \right\| - 1 = 0, \qquad (4.11)$$

with boundary conditions $\forall\, k$:

$$\hat{\boldsymbol{\Omega}}_k(0) = \hat{\boldsymbol{\Omega}}_k^{\text{i}}, \quad \hat{\boldsymbol{\Omega}}_k(1) = \hat{\boldsymbol{\Omega}}_k^{\text{f}} \qquad (4.12)$$

yields equations of motion for the collection of links $\hat{\boldsymbol{\Omega}}_{k=1,\ldots,N}$ with an all-to-all coupling unamenable to analytic methods.

An analytic solution would yield the entire path from one end to the other — but we do not need that much. Rather, we need a recursive expression in the spirit of the one we had for a single-link motion in equation 4.9: given a configuration $\boldsymbol{R}_{\text{lnk}}^{(m)}$, we want a new configuration $\boldsymbol{R}_{\text{lnk}}^{(m+1)}(\boldsymbol{R}_{\text{lnk}}^{(m)})$ that is a short step along the best-guess path $\boldsymbol{R}_{\text{lnk}}^{m \to \text{f}}(\tau)$.

Further, there is no need to require that $\boldsymbol{R}_{\text{lnk}}^{(m+1)}(\boldsymbol{R}_{\text{lnk}}^{(m)})$ lies *exactly* on the best-guess path. A sensible thing to ask for instead is that the distance from $\boldsymbol{R}_{\text{lnk}}^{(m+1)}$ to the path $\boldsymbol{R}_{\text{lnk}}^{m \to \text{f}}(\tau)$ vanishes as $\boldsymbol{R}_{\text{lnk}}^{(m+1)}$ gets closer to $\boldsymbol{R}_{\text{lnk}}^{(m)}$.

We can get at satisfying the above requirement in the following way. The best-guess path $\boldsymbol{R}_{\text{lnk}}^{m \to \text{f}}$ has an affine-linear parameter τ from equation 4.1 (with $b = 0$). According to equation 2.10, a small increment in kinematic length ℓ along the path from $\tau = 0$ to $\tau = \delta\tau$ is given by

$$\delta\ell = \int_0^{\delta\tau} \sqrt{2T(\tau)}\, \mathrm{d}\tau = \mathcal{O}\left((\delta\tau) \right)$$

which means the integrand does not depend on τ. This is an unsurprising consequence of the fact that in the potential energy landscape ensemble, the configuration-space analogue of kinetic energy is conserved along off-boundary path segments.

Therefore, a point $\boldsymbol{R}_{\text{lnk}}^{(m+1)}(\boldsymbol{R}_{\text{lnk}}^{(m)})$ that satisfies our requirement of being close to the path $\boldsymbol{R}_{\text{lnk}}^{m \to \text{f}}$ in the limit of a small step along the path will also satisfy:

$$\frac{1}{2} I_0 \sum_{k,\,l=1}^N D_{kl} \frac{\mathrm{d}\hat{\boldsymbol{\Omega}}_k^{(m+1)}}{\mathrm{d}\tau} \cdot \frac{\mathrm{d}\hat{\boldsymbol{\Omega}}_l^{(m+1)}}{\mathrm{d}\tau} = f(\hat{\boldsymbol{\Omega}}_{k=1,\ldots,N}^{(m)}) + \mathcal{O}\left((\delta\tau)^n \right) \qquad (4.13)$$

where f does not depend on τ and $n > 1$. From here on, we will aim to satisfy this equation through linear order in $\delta\tau$, so that $n = 2$. What follows in this chapter is a report on the work in progress to design an algorithm for computing the off-boundary segments of polymer geodesics based on the idea laid out above.

To put this requirement to use, we propose a recursive ansatz $\hat{\boldsymbol{\Omega}}^{(m+1)}_{k=1,\dots,N}(\hat{\boldsymbol{\Omega}}^{(m)}_{k=1,\dots,N}, \tau)$ — a parameterization that captures the evolution of each link vector. At each step of path propagation, we tune the ansatz parameters so that the kinetic energy at the next step only depends on the configuration at the last step and does not depend on τ through linear order.

We propose the following ansatz:

$$
\begin{cases}
\hat{\boldsymbol{\Omega}}^{(0)} \triangleq \hat{\boldsymbol{\Omega}}^{\mathrm{i}} \\
\hat{\boldsymbol{\Omega}}^{(m+1)} = \cos\left(\delta\theta^{(m)}\right) \hat{\boldsymbol{\Omega}}^{(m+1)}_{\mathrm{S}} + \sin\left(\delta\theta^{(m)}\right) \hat{\boldsymbol{n}}^{(m)} \\
\cos\left(\psi^{(m)}\right) \triangleq \hat{\boldsymbol{\Omega}}^{(m)} \cdot \hat{\boldsymbol{\Omega}}^{\mathrm{f}} \\
\hat{\boldsymbol{n}}^{(m)} \triangleq \frac{\hat{\boldsymbol{\Omega}}^{(m)} \times \hat{\boldsymbol{\Omega}}^{\mathrm{f}}}{\sin\left(\psi^{(m)}\right)}
\end{cases}
\tag{4.14}
$$

and $\hat{\boldsymbol{\Omega}}^{(m+1)}_{\mathrm{S}}$ is calculated according the Slerp procedure given in equation 4.9. With this ansatz, each unit link vector's motion is given by the in-plane component and out-of-plane forays, while the normalization constraint is respected exactly. The planar component of motion is given by Slerp. We can think of $\delta\theta^{(m)}$ as a measure of how far away $\hat{\boldsymbol{\Omega}}^{(m+1)}$ moves from the plane defined by $\hat{\boldsymbol{\Omega}}^{(m)}$ and $\hat{\boldsymbol{\Omega}}^{\mathrm{f}}$.

Further, we would like write $\delta\theta^{(m)}$ as a power series expansion in terms of τ. We can constrain the form of $\delta\theta^{(m)}(\tau)$ by considering the symmetry of the problem: the director ansatz has to be invariant under simultaneous path direction reversal and the swapping of initial and final orientations:

$$
\hat{\boldsymbol{\Omega}}\left(\tau, \hat{\boldsymbol{\Omega}}^{\mathrm{i}}, \hat{\boldsymbol{\Omega}}^{\mathrm{f}}\right) = \hat{\boldsymbol{\Omega}}\left(-\tau, \hat{\boldsymbol{\Omega}}^{\mathrm{f}}, \hat{\boldsymbol{\Omega}}^{\mathrm{i}}\right)
$$

The exact Slerp solution (4.8) has this property; by looking at the ansatz, we can see that to respect the symmetry, $\delta\theta^{(m)}(\tau)$ has to be an odd function ($\hat{\boldsymbol{n}}$ flips sign under the exchange of boundary orientations).

To respect the boundary conditions, $\delta\theta^{(m)}$ has to be 0 if $\hat{\boldsymbol{\Omega}}^{(m)}$ is within sufficiently close to $\hat{\boldsymbol{\Omega}}^{\mathrm{f}}$. With this in mind, we can write $\delta\theta^{(m)}$ as:

$$
\delta\theta^{(m)} =
\begin{cases}
\theta^{(m)}\delta\tau + \mathcal{O}\left((\delta\tau)^3\right), & \psi^{(m)} > \varepsilon \\
0, & \psi^{(m)} \leq \varepsilon
\end{cases}
\tag{4.15}
$$

We need to use equations 4.14 and 4.15 to work out the expression for kinetic energy $T(\boldsymbol{R}^{(m+1)})$. Details are provided in appendix B, and we will only mention key results here.

20

The configuration-space analogue of internal kinetic energy at step $m + 1$ can be broken down into the sum of diagonal terms and off-diagonal terms:

$$T(\hat{\boldsymbol{\Omega}}_{k=1,\ldots,N}^{(m+1)}) = \frac{1}{2} I_0 \left(\sum_{k=1}^{N} D_{kk} T_{kk}^{(m+1)} + \sum_{\substack{k,\,l \\ k \neq l}}^{N} D_{kl} T_{kl}^{(m+1)} \right), \tag{4.16}$$

Given the ansatz, we work out the expression above and require that it be indendent of τ through linear order. From that requirement, we wish to fix the N free parameters θ_k.

Calculating the diagonal terms in polymer's internal kinetic energy, we obtain:

$$\frac{\mathrm{d}\hat{\boldsymbol{\Omega}}_k^{(m+1)}}{\mathrm{d}\tau} \cdot \frac{\mathrm{d}\hat{\boldsymbol{\Omega}}_k^{(m+1)}}{\mathrm{d}\tau} \triangleq T_{kk}^{(m+1)} = (X_0)_{kk}^{(m+1)} + (X_1)_{kk}^{(m+1)} \delta\tau + \mathcal{O}\left((\delta\tau)^2\right), \tag{4.17}$$

where

$$\begin{aligned} (X_0)_{kk}^{(m+1)} &= \left(\theta_k^{(m)}\right)^2 + \left(\psi_k^{(m)}\right)^2 \\ (X_1)_{kk}^{(m+1)} &= 0 \end{aligned} \tag{4.18}$$

Diagonal terms already do not depend on τ through linear order.

To calculate the cross terms, we first define a new quantity $\hat{\boldsymbol{u}}^{(m)}$, a unit vector along the linear velocity of the link vector $\hat{\boldsymbol{\Omega}}^{(m)}$:

$$\hat{\boldsymbol{u}}^{(m)} \triangleq \frac{1}{\psi^{(m)}} \left.\frac{\mathrm{d}\hat{\boldsymbol{\Omega}}_{\mathrm{S}}^{(m+1)}(\tau)}{\mathrm{d}\tau}\right|_{\tau=0} = \frac{1}{\sin\left(\psi^{(m)}\right)} \left(\hat{\boldsymbol{\Omega}}^{\mathrm{f}} - \hat{\boldsymbol{\Omega}}_{\mathrm{S}}^{(m)} \cos\left(\psi^{(m)}\right) \right) \tag{4.19}$$

Using $\hat{\boldsymbol{u}}^{(m)}$, we work out the cross terms of polymer's internal kinetic energy through linear order in τ:

$$\frac{\mathrm{d}\hat{\boldsymbol{\Omega}}_k^{(m+1)}}{\mathrm{d}\tau} \cdot \frac{\mathrm{d}\hat{\boldsymbol{\Omega}}_l^{(m+1)}}{\mathrm{d}\tau} \triangleq T_{kl}^{(m+1)} = (X_0)_{kl}^{(m+1)} + (X_1)_{kl}^{(m+1)} \delta\tau + \mathcal{O}\left((\delta\tau)^2\right), \tag{4.20}$$

where

$$\begin{aligned} (X_0)_{kl} &= \hat{\boldsymbol{n}}_k \cdot \hat{\boldsymbol{n}}_l \left(\theta_k \theta_l\right) \\ &\quad + \hat{\boldsymbol{u}}_k \cdot \hat{\boldsymbol{u}}_l \left(\psi_k \psi_l\right) \\ &\quad + \left(\hat{\boldsymbol{n}}_k \cdot \hat{\boldsymbol{u}}_l \left(\theta_k \psi_l\right) + (k \leftrightarrow l)\right) \\ (X_1)_{kl} &= -\hat{\boldsymbol{\Omega}}_k \cdot \left(\hat{\boldsymbol{n}}_l \theta_l + \hat{\boldsymbol{u}}_l \psi_l\right) \left((\theta_k)^2 + (\psi_k)^2\right) + (k \leftrightarrow l) \end{aligned} \tag{4.21}$$

where the left-hand terms are at the $m + 1$ step, and all the right-hand terms are at the m step; the step superscripts are omitted for readability. The expression is symmetric in indices k, l, and agrees with diagonal element calculations (4.17) when $k = l$: for the same link, vectors $\hat{\boldsymbol{u}}$, $\hat{\boldsymbol{\Omega}}$ and $\hat{\boldsymbol{n}}$ are mutually perpendicular. See figure 4.2 for a schematic summary of link motion according to the proposed algorithm.

In summary, diagonal terms are independent of τ through linear order, whereas the off-diagonal terms, when expanded in powers of τ, generally have a linear term. Using a

power series expansion of $\delta\theta^{(m)} = \theta^{(m)}\delta\tau + \mathcal{O}\left((\delta\tau)^3\right)$, we want to find a solution —
N numerical values $\theta_k^{(m)}$ — such that the kinetic energy in equation 4.16 is conserved
through linear order in $\delta\tau$:

$$\sum_{\substack{k,\,l \\ k\neq l}}^{N} D_{kl}\left(X_1\right)_{kl}^{(m+1)} \delta\tau$$

$$= -\sum_{\substack{k,\,l \\ k\neq l}}^{N} D_{kl}\left(\hat{\boldsymbol{\Omega}}_k \boldsymbol{\cdot} (\hat{\boldsymbol{n}}_l\theta_l + \hat{\boldsymbol{u}}_l\psi_l)\left((\theta_k)^2 + (\psi_k)^2\right) + (k \leftrightarrow l)\right)\delta\tau = 0.$$

Because each term is symmetric in k and l, the above expression is equivalent to:

$$\sum_{\substack{k,\,l \\ k\neq l}}^{N} D_{kl}\left(\hat{\boldsymbol{\Omega}}_k \boldsymbol{\cdot} (\hat{\boldsymbol{n}}_l\theta_l + \hat{\boldsymbol{u}}_l\psi_l)\left(\psi_k^2 + \theta_k^2\right)\right) = 0 \tag{4.22}$$

Again, the superscripts denoting the iteration step in the algorithm are (m) for all quantities in equation 4.22; they are omitted for readability. Once we have the $\theta_k^{(m)}$'s, we have obtained the next configuration of the polymer. If the configuration has a potential energy above the landscape energy, we perform the escape-step procedure. Finally, the obtained configuration becomes the new initial configuration at the next iteration. We continue on until we reach the endpoint.

Equation 4.22 is non-linear with N unknowns — so in the N-dimensional space of all possible values of θ's, there is an $N-1$ dimensional surface all of which points will satisfy equation 4.22. If we wish to continue on with the proposed algorithm, we need a sensible, physically meaningful way to pick a point on that surface.

In the next chapter, we review the progress made in implementing the algorithm described here for a triatomic molecule, and conclude by discussing directions for follow-up work.
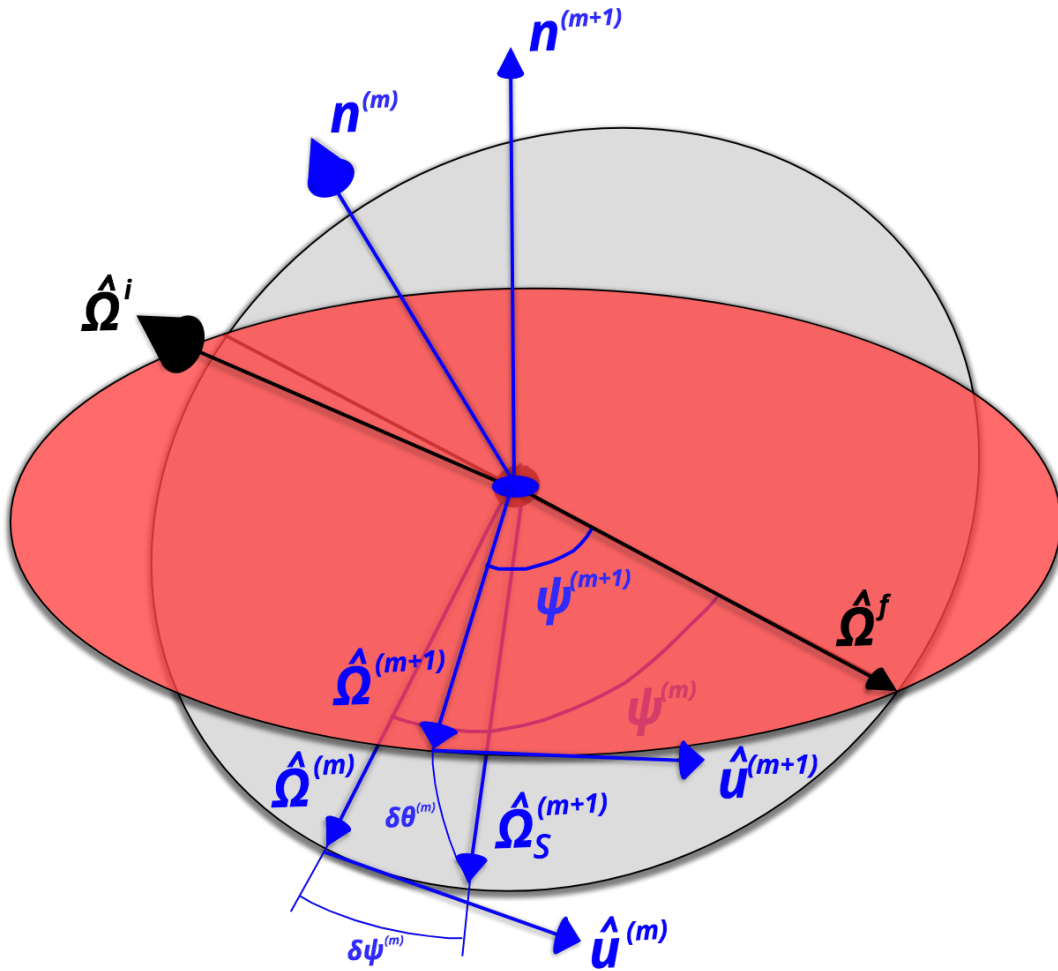
Figure 4.2: A single link vector $\hat{\boldsymbol{\Omega}}$ moving between $\hat{\boldsymbol{\Omega}}^{\mathrm{i}}$ and $\hat{\boldsymbol{\Omega}}^{\mathrm{f}}$ according to the proposed algorithm. At each step m, the link is first moved in the current plane according to the Slerp solution $\hat{\boldsymbol{\Omega}}_{\mathrm{S}}(\tau)$; then the link is pushed out of the plane. The magnitude of the out-of-plane motion is determined by $\delta\theta^{(m)}$. At the beginning of each step m, the in-plane component of the link's linear velocity is directed along the unit vector $\hat{\boldsymbol{u}}^{(m)}$.

Chapter 5

Report on progress and conclusion

When $N = 2$, we can find *a* solution to 4.22

$$\theta_1 = -\frac{\hat{\boldsymbol{u}}_1 \cdot \hat{\boldsymbol{\Omega}}_2}{\hat{\boldsymbol{n}}_1 \cdot \hat{\boldsymbol{\Omega}}_2}\psi_1$$

$$\theta_2 = -\frac{\hat{\boldsymbol{u}}_2 \cdot \hat{\boldsymbol{\Omega}}_1}{\hat{\boldsymbol{n}}_2 \cdot \hat{\boldsymbol{\Omega}}_1}\psi_2$$

(5.1)

The solution corresponds to the case when the two summands of equation 4.22 with $N = 2$ vanish separately.

We examined the trial solution as follows. Using a molecular dynamics simulation for a single triatomic molecule with no potential energy interactions, we obtained MD paths. These MD paths were the initial-value problem solutions to coupled Euler-Lagrange equations subject to normalization constraints on the lengths of the links, but with no constraint on potential energy. Therefore, these paths would look the same as the off-boundary segments of geodesics for the corresponding boundary-value problem, and would coincide with geodesic paths exactly in the limit $E_L \to \infty$. To obtain the corresponding boundary value problem for the geodesic simulation, we used the endpoints of MD paths as an input. We propagated the paths with both the Slerp algorithm 4.9 and the proposed algorithm 4.14. Finally, we computed a few observables along each set of paths. Particularly, we were interested in:

- $\psi_k^{(m)}$ — the angle between $\hat{\boldsymbol{\Omega}}_k^{(m)}$ and $\hat{\boldsymbol{\Omega}}_k^{\mathrm{f}}$ for each link. For the Slerp solution, ψ_k should linearly decrease from the initial value to 0.

- $\hat{\boldsymbol{\Omega}}_k^{(m)} \cdot \hat{\boldsymbol{n}}_k$ — a measure of how much a given link forays out of its original plane defined by $\hat{\boldsymbol{\Omega}}_k^{\mathrm{i}}$ and $\hat{\boldsymbol{\Omega}}_k^{\mathrm{f}}$. For the Slerp solution, the projection of $\hat{\boldsymbol{\Omega}}_k^{(m)}$ onto the normal vector $\hat{\boldsymbol{n}}_k$ should always be zero.

- $\delta\theta_k^{(m)}$ — a measure of how far each $\hat{\boldsymbol{\Omega}}_k^{(m+1)}$ forays of out the *instantaneous* plane defined by $\hat{\boldsymbol{\Omega}}_k^{(m)}$ and $\hat{\boldsymbol{\Omega}}_k^{\mathrm{f}}$.

Figure 5.1: Comparison of $\psi_1^{(m)}$ — the angle between $\hat{\mathbf{\Omega}}_1^{(m)}$ and $\hat{\mathbf{\Omega}}_1^{\mathrm{f}}$ for the first of the two links in the triatomic — given the same set of endpoints and corresponding paths obtained with Slerp, molecular dynamics, and the new algorithm.
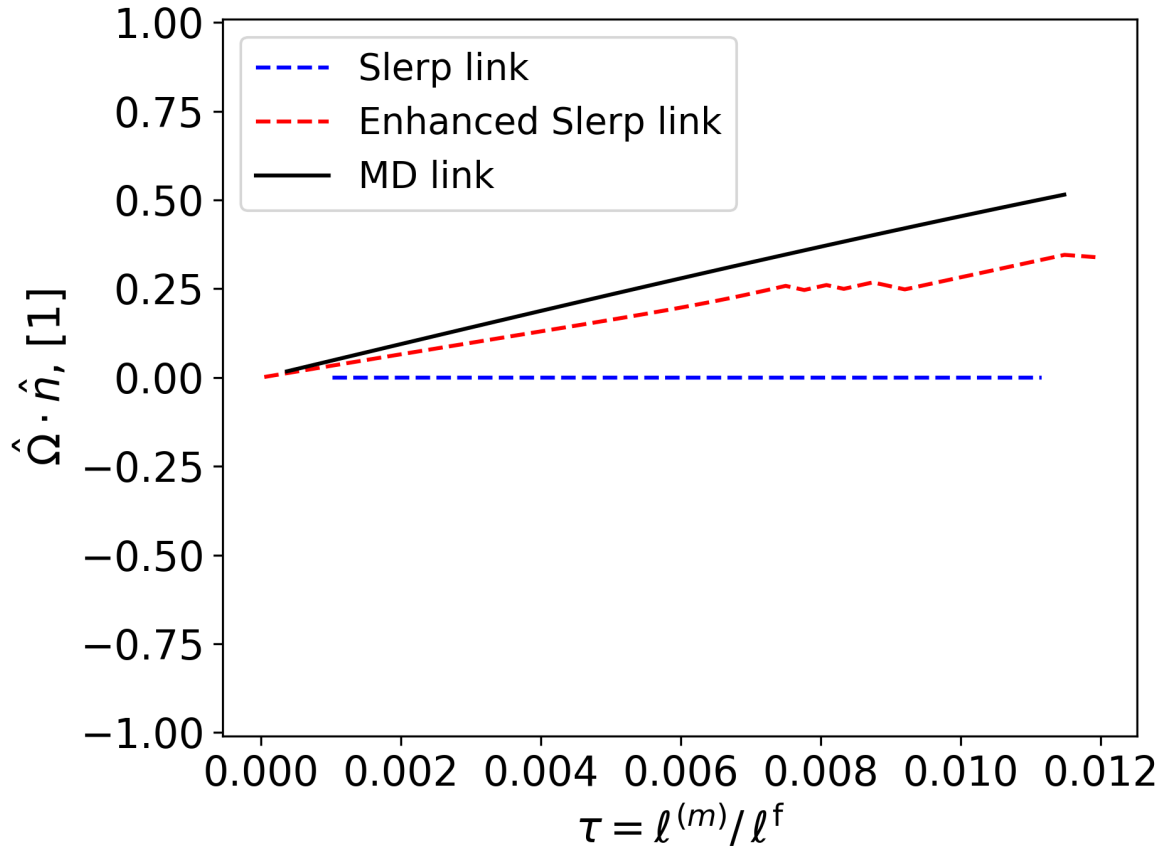
Figure 5.2: Comparison of $\hat{\boldsymbol{\Omega}}_1^{(m)} \cdot \hat{\boldsymbol{n}}_1$ — a measure of how much the first of the two links forays out of its original plane defined by $\hat{\boldsymbol{\Omega}}_1^{\mathrm{i}}$ and $\hat{\boldsymbol{\Omega}}_1^{\mathrm{f}}$ — given the same set of endpoints and corresponding paths obtained with Slerp, molecular dynamics, and the new algorithm.

Figure 5.3: Comparison of $\delta\theta_1^{(m)}$ — a measure of how far $\hat{\mathbf{\Omega}}_1^{(m+1)}$ forays out of the *instantaneous* plane defined by $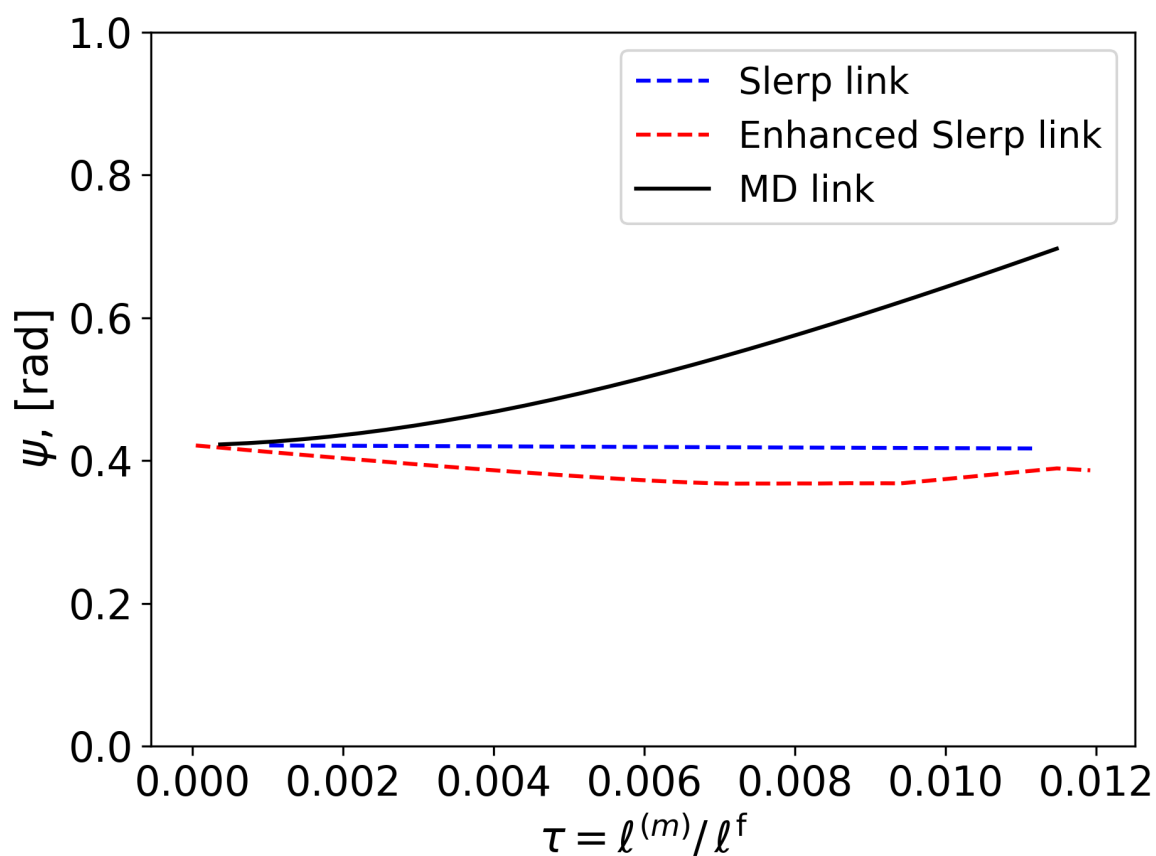\hat{\mathbf{\Omega}}_1^{(m)}$ and $\hat{\mathbf{\Omega}}_1^{\mathrm{f}}$ — given the same set of endpoints and corresponding paths obtained with Slerp, molecular dynamics, and the new algorithm.

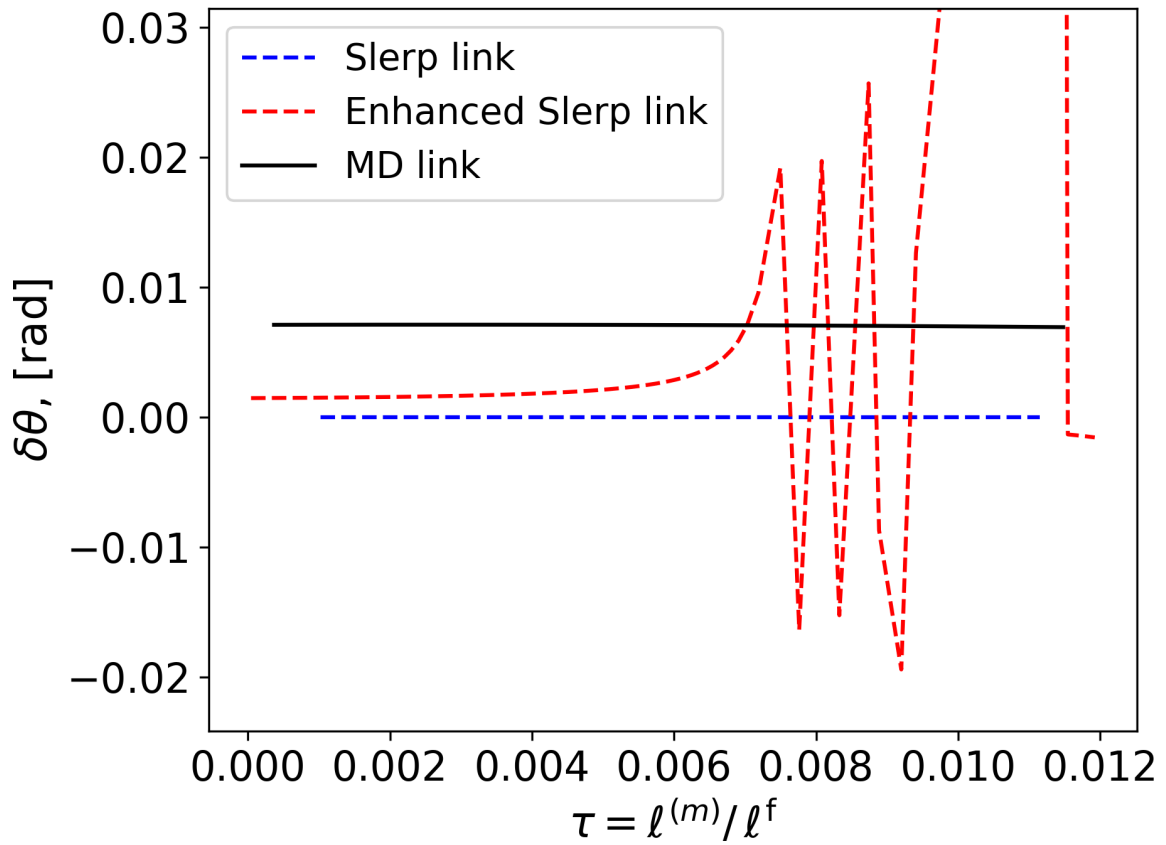In figures 5.1, 5.2, and 5.3, we only show the variables corresponding to the motion of the first link. The motion of the second link is equivalent to that of the first one. Along the x axis of each plot, we measure the progress along any given path as a fraction of its current length $\ell^{(m)}$ to its final length ℓ^{f}. The length of the triatomic's path at step M is calculated as

$$\ell^{(M)} = \sum_{m=1}^{M} \sqrt{\sum_{k=1}^{2} \arccos^2 \left(\hat{\boldsymbol{\Omega}}_k^{(m)} \cdot \hat{\boldsymbol{\Omega}}_k^{(m-1)} \right)}$$

We find that the approach of equation 5.1 does not yield convergent paths: as the scalar product $\hat{\boldsymbol{n}}_1 \cdot \hat{\boldsymbol{\Omega}}_2$ or $(\hat{\boldsymbol{n}}_2 \cdot \hat{\boldsymbol{\Omega}}_1)$ approaches 0 along a path, the parameter θ_1 (or θ_2) becomes singular — see figure 5.3.

We may try to address the issue by finding a new approach to equation 4.22. In doing so, it would be helpful to first test the assumption underlying the current approach 5.1 in the case of a triatomic molecule: that internal kinetic energy of the polymer is not exchanged between the summands of equation 4.22 in the limit of a short step.

Further, we see on figure 5.1 that if the links follow molecular dynamics paths, then $\psi_k(\tau)$ are not monotonically decreasing functions like they are for Slerp paths. In terms of the variables we use in our ansatz 4.14, this non-monotonicity could be a result of either $0 < \delta\psi^{(m)} \leq \left| \delta\theta^{(m)} \right|$ or $\delta\psi^{(m)} < 0$, or both. Since the ansatz 4.14 does not allow in-plane motion away from the final orientation, it may not be able to capture the desired physical behavior even in the limit as the steps along the path get small.

All in all, in solving the problem of coupled-link motion, we have so far attempted analytic approaches. In large, this is because the geodesic algorithm for single-link motion was exact both on its off-boundary and on-boundary segments.[3, 4] Given how complicated the equations of motion become when the links are coupled, and realizing that we only need to solve for a best-guess path along the initial short segment, we tried to formulate a solution for $\boldsymbol{R}^{m \to \mathrm{f}}(\tau)$ that would be exact in the limit of a small step $\delta\tau$. In particular, we proposed an ansatz 4.14 that respected the link normalization constraints exactly.

Perhaps we should think more numerically. We said before that RATTLE cannot be applied to the problem of path propagation because the latter is a boundary value problem while the former is an initial value problem. But we could develop a boundary-value analogue of RATTLE, estimating initial values for velocities at each step from the corresponding *unconstrained* free-geodesic equations. The RATTLE scheme would then approximate the necessary corrections to $\boldsymbol{R}$ at every step to respect the link normalization constraints within specified tolerance.

The idea of geodesic paths in the potential energy landscape ensemble has been incredibly fruitful. In applying this idea to relatively simple systems, it has so far been possible to

approach many aspects of the path-propagation problem exactly.[2–6] Moving forward, we may benefit from adopting more numerical approaches. At the end of the day, a good algorithm is not the one that is most analytically exact; rather, a good algorithm is "good enough" in its approximations for small steps while still finding the shortest many-step path between two points in configuration space.

Bibliography

[1] C. Wang and R. M. Stratt, The Journal of Chemical Physics **127**, 224503 (2007), https://doi.org/10.1063/1.2801994.

[2] C. Wang and R. M. Stratt, The Journal of Chemical Physics **127**, 224504 (2007), https://doi.org/10.1063/1.2801995.

[3] D. Jacobson and R. M. Stratt, The Journal of Chemical Physics **140**, 174503 (2014), https://doi.org/10.1063/1.4872363.

[4] L. Frechette, D. Jacobson, and R. M. Stratt, The Journal of Chemical Physics **141**, 209902 (2014), https://doi.org/10.1063/1.4902974.

[5] L. Frechette and R. M. Stratt, The Journal of Chemical Physics **144**, 234505 (2016), https://doi.org/10.1063/1.4953618.

[6] D. V. Cofer-Shabica and R. M. Stratt, The Journal of Chemical Physics **146**, 214303 (2017), https://doi.org/10.1063/1.4984617.

[7] F. Wiegel, *Introduction to Path-integral Methods in Physics and Polymer Science* (World Scientific, 1986), ISBN 9789971978709.

[8] N. Goldenfeld, *Lectures on phase transitions and the renormalization group*, Frontiers in physics (Addison-Wesley, Advanced Book Program, 1992), ISBN 9780201554083.

[9] M. Stevens, *Polymer Chemistry: An Introduction* (Addison-Wesley Publishing Company, Advanced Book Program, 1975), ISBN 9780201073126.

[10] M. C. Zhang, B.-H. Guo, and J. Xu, Crystals **7** (2017), ISSN 2073-4352, URL http://www.mdpi.com/2073-4352/7/1/4.

[11] A. Coran, in *The Science and Technology of Rubber (Fourth Edition)*, edited by J. E. Mark, , B. Erman, , and C. M. Roland (Academic Press, Boston, 2013), pp. 337 – 381, fourth edition ed., ISBN 978-0-12-394584-6, URL https://www.sciencedirect.com/science/article/pii/B9780123945846000078.

[12] G. E. P. Box, Journal of the American Statistical Association **71**, 791 (1976), `https://doi.org/10.1080/01621459.1976.10480949`.

[13] M. P. Allen and D. J. Tildesley, *Computer Simulation of Liquids* (Oxford University Press, New York, NY, USA, 2017), ISBN 9780198803195.

[14] H. C. Andersen, Journal of Computational Physics **52**, 24 (1983), ISSN 0021-9991, URL `http://www.sciencedirect.com/science/article/pii/0021999183900141`.

[15] K. Shoemake, SIGGRAPH Comput. Graph. **19**, 245 (1985), ISSN 0097-8930, URL `http://doi.acm.org/10.1145/325165.325242`.

Appendix A

Molecular Dynamics Simulation

We have designed a molecular dynamics simulation of a single polymer molecule, modeled as a freely-jointed rigid chain. We used a standard numerical integration scheme, RATTLE, to numerically integrate Euler-Lagrange equations with constraints on the length of each link. The polymer model and the underlying Lennard-Jones potential interactions between the non-neighboring atoms in the chain were introduced in chapter were introduced in chapter 3. In this appendix, we provide the technical details on the imlemented simulation.

Reduced Units and Simulation Parameters

All quantities in the simulation are defined in terms of dimensionless units. In molecular dynamics simulations where potential interactons are included, the relevant units are dictated by the choice of the potential — in our case, the Lennard-Jones potential (see equation 3.1). The LJ potential defines the relevant length scale (σ) and the relevant energy scale (ϵ). Given the etalon mass of the polymer atoms, m, all other quantities follow and are summarized in table A.1. In the molecular dynamics simulations where potential interactions were excluded, the unit of mass m_0, the length of each link d, and the kinetic temperature of the system upon initialization T_0 defined the units. These dimensionless units are summarized in table A.2

The parameters used in the simulation are defined in terms of these units. In simulations with a LJ potential, the relevant parameters are: the mass of polymer atoms m_0, the strength of their interaction ϵ, their effective "diameter"σ, the length of each link d, and the size of the timestep δt. In addition, RATTLE requires to specify the dimensionless tolerance parameter ξ. This parameter determines the allowed relative error in the length of each link from the fixed value (d). In simulations without a LJ potential, the set of parameters was smaller as we did not need to specify either σ or ϵ. The remaining

Table A.1: Dimensionless units in MD simulations with a LJ potential. The units are induced by the unit of mass m_0, and the length and energy scale of the LJ potential, σ_0 and ϵ_0.

Dimensionless Unit	Meausures
$r^* = r/\sigma_0$	distance
$E^* = E/\epsilon_0$	energy
$m^* = m/m_0$	mass
$t^* = t\sqrt{\frac{\epsilon_0}{m_0\sigma_0^2}}$	time
$T^* = k_{\mathrm{B}}T/\epsilon_0$	temperature

Table A.2: Dimensionless units in MD simulations without a LJ potential. The units are induced by the units of mass m_0, and the length of each polymer link d and the initial kinetic temperature of the system, T_0.

Dimensionless Unit	Meausures
$r^* = r/d$	distance
$E^* = E/k_{\mathrm{B}}T_0$	energy
$m^* = m/m_0$	mass
$t^* = t\sqrt{\frac{k_{\mathrm{B}}T_0}{m_0(2\pi d)^2}}$	time
$T^* = T/T_0$	temperature

parameters were the same. The values of parameters are summarized in tables A.3 and A.4.

Throughout our work, we used a variable number of links in the polymer chain (N). For testing thermodynamic averages in the MD simulation, we used $N = 100$, unless indicated otherwise on the relevant figures. For testing our geodesic algorithm, we have so far used a triatomic molecule $N = 2$.

Table A.3: Values of parameters in MD simulations with a LJ potential in dimensionless units as summarized in table A.1.

Parameter	Value
polymer atom mass m	1.0
strength of interatomic interaction ϵ	1.0
effective atomic diameter σ	1.0
link length d	0.85
time step δt	0.001
RATTLE tolerance ξ	$(0.001)^2$

Table A.4: Values of parameters in MD simulations without a potential in dimensionless units as summarized in table A.1.

Parameter	Value
polymer atom mass m	1.0
link length d	1.0
time step δt	0.001
RATTLE tolerance ξ	$(0.001)^2$

A note on initialization and attaining thermodynamic equilibrium

To set up a MD simulation, we initialized the polymer molecule using its link-vector representation, positioning its center of mass at the origin and assigning each link an orientation in three-dimensional space. The orientation of each link was determined by sampling the polar-coordinate angles ϕ and θ uniformly at random. In MD simulations with a LJ potential, once a trial oritentation for another link was determined, we checked whether it led to an overlap of polymer atoms between already-oriented links. If it did, we attempted another trial orientation for the link.

Once the configuration of the links was determined, the directions of link velocities were similarly assigned at random, and then corrected to be perpendicular to the orientation of the respective link. The speeds were sampled from an exponential distribution and scaled to yield the desired temperature.

Note: we have not yet performed the whole range of necessary experiments to ensure our system attains thermodynamic equilibrium. It is possible that single polymer molecule, modeled as a freely jointed rigid chain, will not equilibrate at all. To attain equilibrium, it would be helpful to submerge the polymer in a solution, facilitating equilibration by having the polymer interact with solvent molecules. To that end, we have also built a MD simulation of a Lennard-Jones atomic liquid. In the future, when the geodesic-finding algorithm for polymers is developed, a well-equilibrated system will be necessary to provide the input configuration-space points to the geodesic algorithm.

Testing energy and angular momentum conservation

We tested that over the course of our MD simulation, energy and angular momentum are conserved. To test that constraint forces in RATTLE were properly implemented, we also verified that the virial-theorem estimate of average kinetic energy converged to the average kinetic energy calculated directly from atomic velocities.
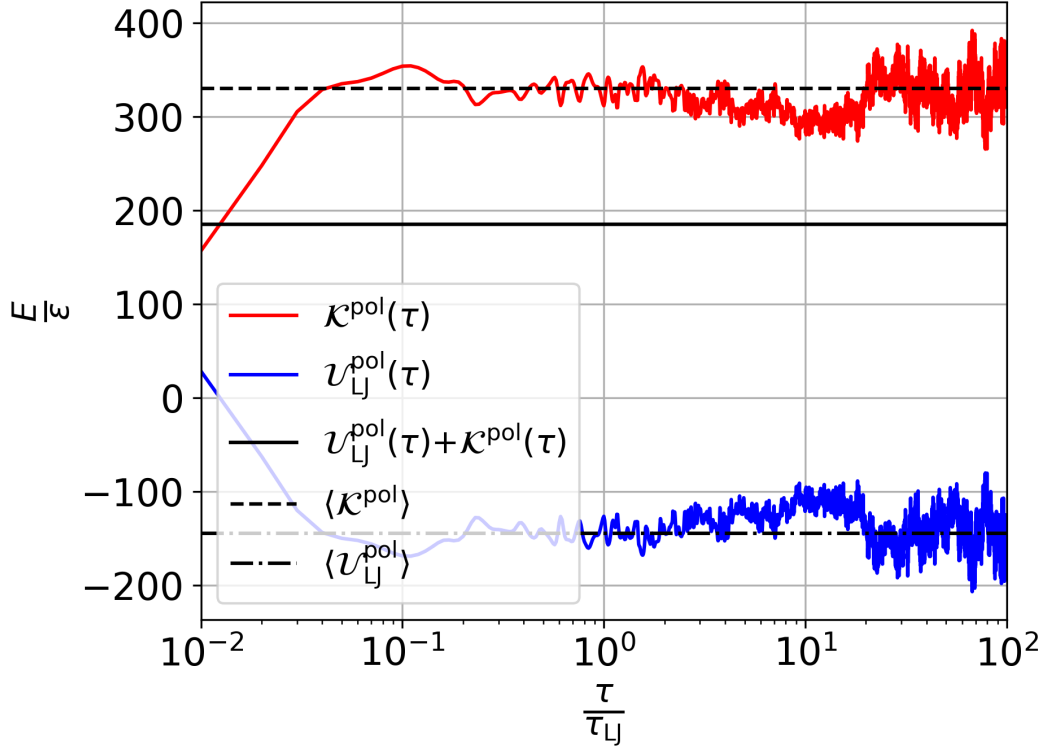
Figure A.1: A test of energy conservation for a MD simulation of a $N = 100$ link chain with a LJ potential.

The virial theorem is a statement from classical mechanics that, given a stable system of N particles bound by potential forces, relates the system's time average of kinetic energy, $\langle T \rangle$, to the system's time average of potential energy:

$$\langle T \rangle = -\frac{1}{2} \sum_{k=1}^{N} \langle \boldsymbol{F}_k \boldsymbol{\cdot} \boldsymbol{r}_k \rangle \tag{A.1}$$

where $\boldsymbol{F}_k$, $\boldsymbol{r}_k$ denote a total force on and a position of the kth particle, respectively. On the right-hand side of the equation, the time average of the system's potential energy is expressed in terms of the quantity called a *virial*. In the case of our polymer model, at any point in time the total force on a given atom k is a vector sum of a total force $\boldsymbol{F}_k$ due to the Lennard-Jones potential and the total constraint force $\boldsymbol{G}_k$. On figure A.3, we denote

$$\mathcal{W}_{\mathrm{LJ}} = \sum_{k=1}^{N} \boldsymbol{F}_k \boldsymbol{\cdot} \boldsymbol{r}_k$$

$$\mathcal{W}_{\mathrm{C}} = \sum_{k=1}^{N} \boldsymbol{G}_k \boldsymbol{\cdot} \boldsymbol{r}_k$$

The tests are summarized in the three figures that follow in this section.
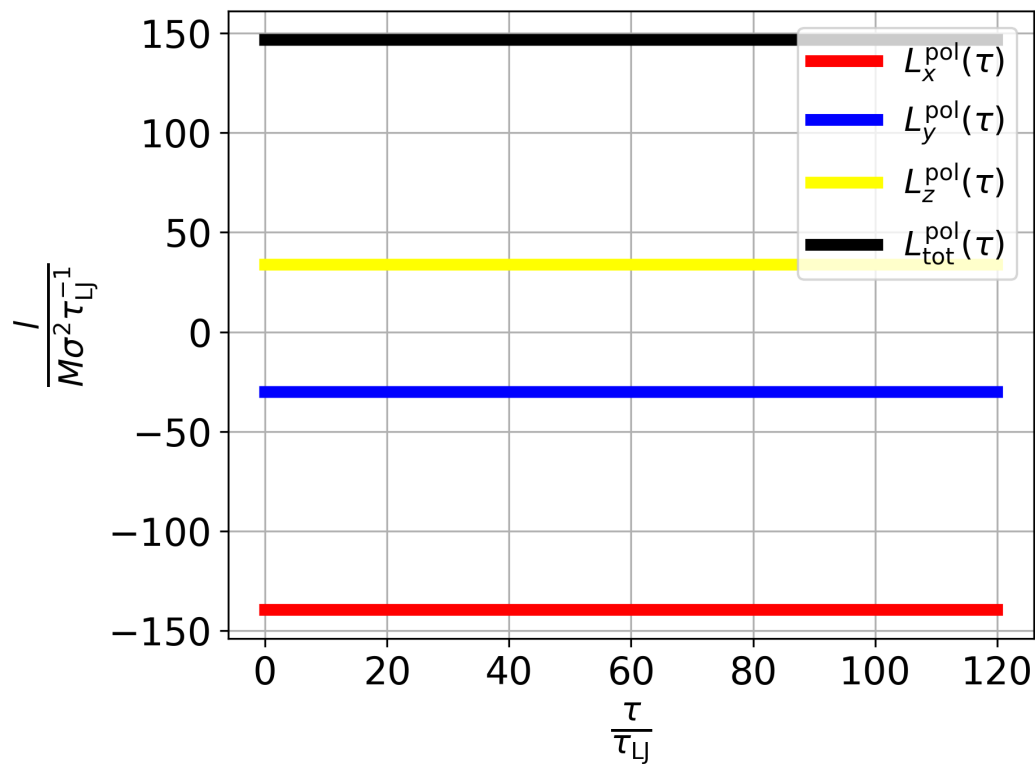
Figure A.2: A test of angular momentum conservation for a MD simulation of a $N = 100$ link chain with a LJ potential.
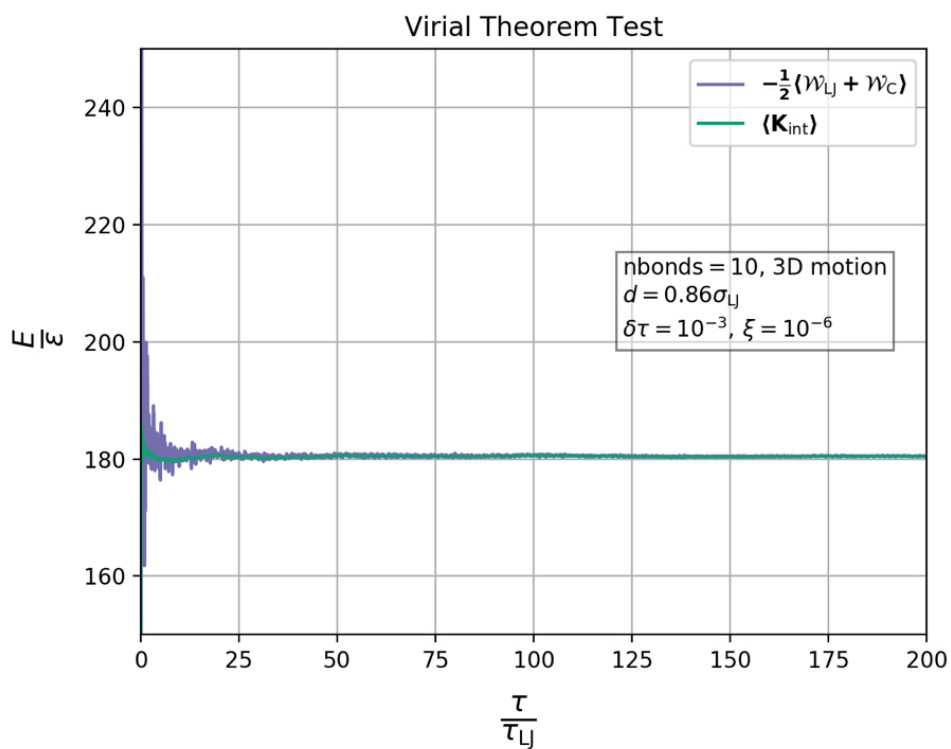
Figure A.3: A virial-theorem estimate of average kinetic energy converged to the average kinetic energy calculated directly from atomic velocities. The virial comprises the contributions from both Lennard-Jones and RATTLE constraint forces.

Appendix B

Kinetic Energy of the Polymer

In this appendix, we include calculations pertinent to the kinetic energy of the polymer in the link-vector representation as well as the derivation of the kinetic energy conservation condition.

First, note: any atomic position vector in the polymer molecule $\boldsymbol{r}_i$, $i > 0$, can be found by following the bond vectors from the beginning of the chain:

$$\boldsymbol{r}_i = \boldsymbol{r}_0 + \sum_{j=1}^{i} d\hat{\boldsymbol{\Omega}}_j \tag{B.1}$$

Therefore, we can write $\boldsymbol{r}_{\mathrm{CM}}$ as

$$\boldsymbol{r}_{\mathrm{CM}} = \boldsymbol{r}_0 + \frac{d}{N+1} \sum_{i=1}^{N} (N+1-i)\hat{\boldsymbol{\Omega}}_i \tag{B.2}$$

And $\boldsymbol{v}_{\mathrm{CM}}$ is given by

$$\boldsymbol{v}_{\mathrm{CM}} = \boldsymbol{v}_0 + \frac{d}{N+1} \sum_{i=1}^{N} (N+1-i)\dot{\hat{\boldsymbol{\Omega}}}_i \tag{B.3}$$

In the link-vector representation, we can express the position and velocity of the first atom, $\boldsymbol{r}_0$ and $\boldsymbol{v}_0$, with equations B.2 and B.3.

To obtain the link-vector representation of the kinetic energy, we start with the expression for the velocity of the ith atom in the molecule relative to $\boldsymbol{v}_{\mathrm{CM}}$ ($i \geq 1$):

$$\boldsymbol{v}_i - \boldsymbol{v}_{\mathrm{CM}} = \left(\boldsymbol{v}_0 + d\sum_{j=1}^{i} \dot{\hat{\boldsymbol{\Omega}}}_j \right) - \left(\boldsymbol{v}_0 + \frac{d}{N+1} \sum_{i=1}^{N} (N+1-i)\dot{\hat{\boldsymbol{\Omega}}}_i \right)$$

$$= d\sum_{j=1}^{i} \dot{\hat{\boldsymbol{\Omega}}}_j - \frac{d}{N+1} \sum_{j=1}^{N} (N+1-j)\, \dot{\hat{\boldsymbol{\Omega}}}_j$$

The term $(\boldsymbol{v}_0 - \boldsymbol{v}_{\mathrm{CM}})$ is given by

$$\boldsymbol{v}_0 - \boldsymbol{v}_{\mathrm{CM}} = -\frac{d}{N+1}\sum_{i=1}^{N}(N+1-i)\dot{\hat{\boldsymbol{\Omega}}}_i$$

Squaring the expression and summing over all the atoms gives:

$$\sum_{i=0}^{N}(\boldsymbol{v}_i - \boldsymbol{v}_{\mathrm{CM}})^2 = \left(\frac{d}{N+1}\right)^2 \sum_{j,\,k=1}^{N} B_{jk}\dot{\hat{\boldsymbol{\Omega}}}_j \boldsymbol{\cdot} \dot{\hat{\boldsymbol{\Omega}}}_k$$

$$+ d^2\sum_{i=1}^{N}\left(\left(\sum_{j=1}^{i}\dot{\hat{\boldsymbol{\Omega}}}_j\right)^2 + \left(\frac{1}{N+1}\right)^2 \sum_{j,\,k=1}^{N} B_{jk}\dot{\hat{\boldsymbol{\Omega}}}_j \boldsymbol{\cdot} \dot{\hat{\boldsymbol{\Omega}}}_k - \frac{2}{N+1}\sum_{j=1}^{N}\left(A_j\dot{\hat{\boldsymbol{\Omega}}}_j\right)\left(\sum_{k=1}^{i}\dot{\hat{\boldsymbol{\Omega}}}_k\right)\right)$$

Where $A_j = (N+1-j)$ and $B_{jk} = (N+1-j)(N+1-k)$.

The second term in the expression, when summed over the N links, gives

$$d^2\sum_{i=1}^{N}\left(\sum_{j=1}^{i}\dot{\hat{\boldsymbol{\Omega}}}_j\right)^2 = \sum_{i=1}^{N} d^2\left(\sum_{j=1}^{i}\dot{\hat{\boldsymbol{\Omega}}}_j\right)\left(\sum_{k=1}^{i}\dot{\hat{\boldsymbol{\Omega}}}_k\right)$$

$$= d^2\sum_{j=1}^{N}\sum_{k=1}^{N}\left(N+1-\max(j,\,k)\right)\dot{\hat{\boldsymbol{\Omega}}}_j \boldsymbol{\cdot} \dot{\hat{\boldsymbol{\Omega}}}_k$$

The first and third terms in the expression do not have free indices, so summing over simply gives $N+1$ identical terms.

Summing the fourth term in the expression above, we obtain

$$-d^2\frac{2}{N+1}\sum_{i=1}^{N}\left(\sum_{j=1}^{N}A_j\dot{\hat{\boldsymbol{\Omega}}}_j\right)\left(\sum_{k=1}^{i}\dot{\hat{\boldsymbol{\Omega}}}_k\right) = -d^2\frac{2}{N+1}\sum_{j=1}^{N}\sum_{k=1}^{N}(N+1-j)(N+1-k)\dot{\hat{\boldsymbol{\Omega}}}_j \boldsymbol{\cdot} \dot{\hat{\boldsymbol{\Omega}}}_k$$

$$= -d^2\frac{2}{N+1}\sum_{j,\,k=1}^{N} B_{jk}\dot{\hat{\boldsymbol{\Omega}}}_j \boldsymbol{\cdot} \dot{\hat{\boldsymbol{\Omega}}}_k$$

Combining all the terms, we obtain:

$$\sum_{i=0}^{N}(\boldsymbol{v}_i - \boldsymbol{v}_{\mathrm{CM}})^2 = d^2\sum_{j=1}^{N}\sum_{k=1}^{N}\left(\left(N+1-\max(j,\,k)\right)\dot{\hat{\boldsymbol{\Omega}}}_j \boldsymbol{\cdot} \dot{\hat{\boldsymbol{\Omega}}}_k + \frac{1}{N+1}B_{jk}\dot{\hat{\boldsymbol{\Omega}}}_j \boldsymbol{\cdot} \dot{\hat{\boldsymbol{\Omega}}}_k - \frac{2}{N+1}B_{jk}\dot{\hat{\boldsymbol{\Omega}}}_j \boldsymbol{\cdot} \dot{\hat{\boldsymbol{\Omega}}}_k\right)$$

$$= d^2\sum_{j=1}^{N}\sum_{k=1}^{N}\left(\left(N+1-\max(j,\,k) - \frac{(N+1-j)(N+1-k)}{N+1}\right)\dot{\hat{\boldsymbol{\Omega}}}^j \boldsymbol{\cdot} \dot{\hat{\boldsymbol{\Omega}}}^k\right)$$

$$= \frac{d^2}{N+1}\sum_{j=1}^{N}\sum_{k=1}^{N}\left(\left(\min(j,\,k)(N+1) - jk\right)\dot{\hat{\boldsymbol{\Omega}}}_j \boldsymbol{\cdot} \dot{\hat{\boldsymbol{\Omega}}}_k\right)$$

$$= d^2\left(\sum_{j,\,k=1}^{N} D_{jk}\dot{\hat{\boldsymbol{\Omega}}}_j \boldsymbol{\cdot} \dot{\hat{\boldsymbol{\Omega}}}_k\right)$$

Where we defined a matrix D_{jk}:

$$D_{jk} = \frac{\min(j,\,k)(N+1) - jk}{N+1}$$

This yields an expression for the internal kinetic energy of the system:

$$T_{\text{internal}} = \frac{1}{2}(N+1)md^2 \sum_{j,\,k=1}^{N} D_{jk}\dot{\hat{\boldsymbol{\Omega}}}_j \cdot \dot{\hat{\boldsymbol{\Omega}}}_k$$

To derive the kinetic energy conservation condition, we provide the necessary auxiliary calculations below in this appendix.

$$\frac{\mathrm{d}\hat{\boldsymbol{\Omega}}^{(m+1)}}{\mathrm{d}\tau} = -\frac{\mathrm{d}\left(\delta\theta^{(m)}\right)}{\mathrm{d}\tau}\sin\left(\delta\theta^{(m)}\right)\hat{\boldsymbol{\Omega}}_{\mathrm{S}}^{(m+1)} + \frac{\mathrm{d}\left(\delta\theta^{(m)}\right)}{\mathrm{d}\tau}\cos\left(\delta\theta^{(m)}\right)\hat{\boldsymbol{n}}^{(m)} + \cos\left(\delta\theta^{(m)}\right)\frac{\mathrm{d}\hat{\boldsymbol{\Omega}}_{\mathrm{S}}^{(m+1)}}{\mathrm{d}\tau}$$
$$(\text{B.4})$$

We have a circular motion along the arc between the initial and final orientations of each link; for the in-plane (Slerp) component of the motion, the angular velocity vector is along $\hat{\boldsymbol{n}}^{(m)}$, and the linear velocity is along the vector $\frac{\mathrm{d}\hat{\boldsymbol{\Omega}}_{\mathrm{S}}^{(m+1)}}{\mathrm{d}\tau}$, which is given by

$$\frac{\mathrm{d}\hat{\boldsymbol{\Omega}}_{\mathrm{S}}^{(m+1)}}{\mathrm{d}\tau} = -\psi^{(m)}\frac{\cos\left(\psi^{(m)}\left(1-\tau\right)\right)}{\sin\left(\psi^{(m)}\right)}\hat{\boldsymbol{\Omega}}_{\mathrm{S}}^{(m)} + \psi^{(m)}\frac{\cos\left(\psi^{(m)}\tau\right)}{\sin\left(\psi^{(m)}\right)}\hat{\boldsymbol{\Omega}}^{\mathrm{f}} \qquad (\text{B.5})$$

In subsequent calculations, we will Taylor expand $\hat{\boldsymbol{\Omega}}_{\mathrm{S}}^{(m+1)}$ and $\frac{\mathrm{d}\hat{\boldsymbol{\Omega}}_{\mathrm{S}}^{(m+1)}}{\mathrm{d}\tau}$ around $\tau = 0$. We denote

$$\hat{\boldsymbol{u}}^{(m)} \triangleq \frac{1}{\psi^{(m)}}\frac{\mathrm{d}\hat{\boldsymbol{\Omega}}_{\mathrm{S}}^{(m+1)}}{\mathrm{d}\tau}\bigg|_{\tau=0} = \frac{1}{\sin\left(\psi^{(m)}\right)}\left(\hat{\boldsymbol{\Omega}}^{\mathrm{f}} - \hat{\boldsymbol{\Omega}}_{\mathrm{S}}^{(m)}\cos\left(\psi^{(m)}\right)\right) \qquad (\text{B.6})$$

Note that vectors $\hat{\boldsymbol{n}}_k$, $\hat{\boldsymbol{u}}_k$, and $\hat{\boldsymbol{\Omega}}_k$ are mutually perprendicular. This can also be seen on figure 4.2. Using this relationship between the three vectors and expression in equation B.4, one computes the diagonal and off-diagonal dot products through linear order in $\delta\tau$ to obtain the derived expressions 4.18 and 4.21.